

November 2021

Copper Electrodeposition Assisted by Hydrogen Evolution for Wearable Electronics: Interconnections and Fiber Metallization

Sabrina M. Rosa Ortiz
University of South Florida

Follow this and additional works at: <https://digitalcommons.usf.edu/etd>



Part of the [Electrical and Computer Engineering Commons](#)

Scholar Commons Citation

Rosa Ortiz, Sabrina M., "Copper Electrodeposition Assisted by Hydrogen Evolution for Wearable Electronics: Interconnections and Fiber Metallization" (2021). *USF Tampa Graduate Theses and Dissertations*.

<https://digitalcommons.usf.edu/etd/9220>

This Dissertation is brought to you for free and open access by the USF Graduate Theses and Dissertations at Digital Commons @ University of South Florida. It has been accepted for inclusion in USF Tampa Graduate Theses and Dissertations by an authorized administrator of Digital Commons @ University of South Florida. For more information, please contact digitalcommons@usf.edu.

Copper Electrodeposition Assisted by Hydrogen Evolution for Wearable
Electronics: Interconnections and Fiber Metallization

by

Sabrina M. Rosa-Ortiz

A dissertation submitted in partial fulfillment
of the requirements for the degree of
Doctor of Philosophy
Department of Electrical Engineering
College of Engineering
University of South Florida

Major Professor: Arash Takshi, Ph.D.
Sylvia Thomas, Ph.D.
Jing Wang, Ph.D.
Sarah Ying Zhong, Ph.D.
Theresa Evans-Nguyen, Ph.D.

Date of Approval:
May 3, 2021

Keywords: Hydrogen Evolution Assisted Electroplating, Multiwall Carbon Nanotubes,
Electronic Devices, Printed Circuit Boards

Copyright © 2021, Sabrina M. Rosa-Ortiz

Dedication

This dissertation is dedicated to myself for not giving up even in the hardest time, for having the necessary strength to continue, for always believing in that dream that one day I had as a child and for seeing that with dedication and desire, everything can be achieved, to my parents, Luis and María, to my brother Saúl, my boyfriend Alejandro, my son Julien, and my dearest friend Pablo for always being my support system, for taking care of me and for always give me the most real advice, to Bernard Batson and Dr. Arash Takshi for believing in me and for giving me advice in the most difficult moments, and to Dr. Sylvia Thomas for inspiring me as a woman and as a professional.

Acknowledgments

During my 5 years as a graduate student at the University of South Florida many colleagues, professors and peers have helped me to make this dissertation possible. I would like to thank Bernard Batson for always providing help in financial support, for promoting my professional development and for all your support during these years. To my mentor Dr. Arash Takshi for allowing me to explore and create in our research lab and allowing me to find my own way, for always giving me advice and ensuring I stayed on the right path, for understanding and giving support throughout every difficult time I have gone throughout these years. To my colleague Dr. Radwan Elzein for always being there if I needed help in class or if I had questions about the research carried out in the laboratory and the instruments. To my colleagues Dr. Belqasem Aljafari, Dr. Fatemeh Khorramshahi, Kishore and Aditya for helping me with the instruments, synthesis, for all the support in difficult times and for taking out of your time when I had doubts. To Dr. Emirov for always take time to explain the procedures of each characterization instrument that I have doubts about and always be ready to take images of my samples. To William Serrano for all his support throughout my grad school application and during those first years as a graduate student where life was not so easy for me. To Dr. Luis Rosa for encouraging me to attend grad school, but more important for being a mentor in the most difficult times when I thought that it was not possible for me to achieve my goal of obtaining a PhD, thank you for believing in me and for motivating me to always give my best. To Bahamundi, Gerena, Jiménez, Ríos, Hernández, and Solís for always believing in my potential as a student, for giving me the necessary tools for my development as a student, and for making science an important part of my life. To my family for

always being there. Without all these people I would not be here today, and I would have given up when I thought I could not continue this journey. Each of these people have contributed to my professional but also personal development, they have taught me that there is only one life, and we must get the most out of it if within our reach.

Table of Contents

List of Tables	iii
List of Figures	iv
Abstract	vii
Chapter 1: Introduction	1
Chapter 2: Background	5
2.1 Literature Review	8
Chapter 3: Low Temperature Soldering Surface-Mount Electronic Components with Hydrogen Assisted Copper Electroplating	12
3.1 Introduction	12
3.2 Experimental	13
3.3 Results and Discussion	14
3.4 Conclusion	17
Chapter 4: Study the Impact of CuSO_4 and H_2SO_4 Concentrations on Lateral Growth of Hydrogen Evolution Assisted Copper Electroplating	18
4.1 Introduction	18
4.2 Experimental	20
4.3 Results and Discussion	22
4.4 Conclusion	32
Chapter 5: Copper Electrodeposition by Hydrogen Evolution Assisted Electroplating (HEA) for Wearable Electronics	34
5.1 Introduction	34
5.2 Experimental	36
5.2.1 Materials	36
5.2.1.1 Textiles	36
5.2.1.2 Interconnection Track	37
5.2.1.3 Electrolyte	37
5.2.2 Sample Preparation	37
5.3 Results and Discussion	38
5.4 Conclusion	42

Chapter 6: Advances in Lateral Copper Electroplated Metallic Tracks:	
Production and Applications by Using Hydrogen Evolution Assisted Electroplating	44
6.1 Introduction.....	44
6.2 Experimental.....	46
6.3 Results and Discussion	47
6.4 Conclusion	51
Chapter 7: Hydrogen Evolution Assisted Cyclic Electroplating for Lateral Copper	
Growth in Wearable Electronics	52
7.1 Introduction.....	52
7.2 Experimental.....	54
7.2.1 Electrochemical Cell and Sample Preparation.....	54
7.2.2 Electrochemical and Electrical Measurements	55
7.2.3 Morphology Analysis.....	55
7.3 Results and Discussion	55
7.4 Conclusion	61
Chapter 8: Conclusion and Suggestions for Future Work	63
8.1 Conclusion	63
8.2 Future Work.....	64
8.2.1 Triaxial Braided Piezo Electric Fibers.....	64
8.2.2 Incorporation of Conductive Fibers over Textiles	
to Improve Flexibility and Conduct Copper Electrodeposition	66
8.2.3 Nozzle for Direct Copper Electrodeposition.....	67
References.....	68
Appendix A: Copyright Permissions	75

List of Tables

Table 1. Types of Electrochemical cells	5
Table 2. Electrodeposition techniques	8
Table 3. Different methods of fabricating e-textiles	36
Table 4. Conductivity measurements for fabrics before and after the copper electrodeposition	47

List of Figures

Figure 1. Schematic diagram of the electrochemical cell employing the redox reaction and hydrogen evolution assisted electroplating	6
Figure 2. PCB sample was used to study HEA copper electroplating across the gap	14
Figure 3. Images of the HEA electroplating across a 1 mm gap on a PCB sample.....	15
Figure 4. Current versus time during the electroplating of the PCB sample	16
Figure 5. Images of the low temperature soldering of a surface mount LED (a) before and (b) after the HEA copper electroplating	16
Figure 6. Schematic of the patterned electrodes on a PCB and the O-ring area for the electrochemical cell.....	22
Figure 7. Images of copper deposition with a magnification of 21× using hydrogen evolution assisted (HEA) electroplating for 0.15 M CuSO ₄ in 1.0 M H ₂ SO ₄ : a) before, b) during (30 s after starting), and c) after electroplating (67.8 s electroplating duration)	23
Figure 8. a) Electrodeposition current (A) vs. time (s) and b) current between the cathodes vs. time (s) for the electrolyte containing 0.15 M CuSO ₄ and 1.0 M H ₂ SO ₄	24
Figure 9. Lateral growth rate (μm s ⁻¹) vs. acid concentrations (M) for 0.15 M CuSO ₄	25
Figure 10. Holes made of copper deposits after hydrogen evolution assisted (HEA) electroplating for concentrations of 0.15 M CuSO ₄ (a, c) in 0.125 M H ₂ SO ₄ and (b, d) in 1.0 M H ₂ SO ₄	27
Figure 11. a) Cyclic voltammetry result for 0.15 M CuSO ₄ and 1.0 M H ₂ SO ₄ , b) Adhesion test of the sample using a transparent Scotch tape showing the pictures before and after the test	29

Figure 12. Light emitting diode (LED) configuration, a) LED over working electrode with gap for copper electrodeposition, b) copper junction between LED and working electrode after copper electrodeposition assisted by hydrogen evolution, c) light emitting diode (LED) configuration after applying a voltage using Keithley 2602A & d) electrochemical growth current during soldering the LED	30
Figure 13. A schematic of a piece of fabric with MWCNT track and connection cables properly sewed to provide continuous connection between the fabric and the instrument	38
Figure 14. a) 1000 Denier Coated Cordura Nylon and b) Laminated Polyester Ripstop fabrics before and after copper electrodeposition takes place	39
Figure 15. Structure of the Laminated Polyester Ripstop fabric at 100 μm	40
Figure 16. a) 1000 Denier Coated Cordura Nylon at 50 μm showing copper with a cauliflower structure after deposition and b) Laminated Polyester Ripstop fabrics after copper electrodeposition showing a more uniform structure with some copper agglomeration	40
Figure 17. Optical microscope image of the 100% Virgin Vinyl fabric with the MWCNTs conductive template a) before and b) during the electroplating process.....	48
Figure 18. Optical microscope image of the Laminated Polyester Ripstop fabric with the MWCNTs conductive template a) before and b) during the electroplating process	48
Figure 19. Optical microscope image of the 1000 Denier Coated Cordura Nylon fabric with the MWCNTs conductive template a) before and b) during the electroplating process.....	49
Figure 20. a) Observation of dendrite and cauliflower formations over a 1000 Denier Coated Cordura Nylon fabric at 100 μm using an SEM Hitachi S-800, b) Cauliflower structure of 1000 Denier Coated Cordura Nylon fabric at 50 μm	50
Figure 21. Cyclic voltammetry result for 1000 Denier Coated Cordura Nylon, Laminated Polyester Ripstop and 100% Virgin Vinyl	51
Figure 22. a) Schematic of the working and counter electrodes on a PCB, b) schematic of the connection of the electrodes with the VersaStat 4.0 instrument, c) lateral growth before and after the copper electrodeposition	54
Figure 23. CV results for the samples grown between -0.8 V and -1.3 V	56

Figure 24. Copper lateral growth rate vs. the frequency of the AC for different V_{DC} and V_{AC} amplitudes as defined in cases a-d.....	57
Figure 25. Selected SEM images of different samples associated to their growth conditions	59
Figure 26. The voltage variation in cases ‘a’, ‘b’, ‘c’, and ‘d’	61
Figure 27. a) Triaxial braided piezo fiber, b) braided PVDF with inner silver coated nylon, c) triaxial braided piezo fiber with MWCNTs ink used for the hydrogen evolution assisted electroplating showing a higher porosity structure, d) triaxial braided piezo fiber without MWCNTs after deposition.....	65
Figure 28. Schematic of the electrochemical cell	66
Figure 29. Integration of fibers on a flexible substrate (fabric or polymer) to conduct the copper electroplating technique	66
Figure 30. Nozzle Set-up	67

Abstract

The current project focused on studying an innovative and novel method, called hydrogen evolution assisted (HEA) electroplating, for rapid and localized electrochemical copper deposition that can be applied for integration of electronic circuits to printed circuit boards (PCBs) and fabrics for developing smart textile (e-textile) and advanced wearable electronics. This method has shown a great enhancement to the deposition rate of copper compared to the conventional galvanostatic electroplating method, opening new venues for patterning conductive circuit layouts on fabrics and for the direct integration of devices into fabrics. While due to the slow growth rate and low mechanical flexibility of copper, the conventional electrodeposition has not been much studied for wearable electronics, our new HEA electroplating method addresses both issues.

Our preliminary studies on HEA electroplating showed the feasibility of growing copper laterally across a 1 mm gap between two copper cathodes (~4 mm wide) that were patterned on a FR-4 printed circuit board (PCB) substrate by the usage of an acidic electrolyte made of H_2SO_4 and CuSO_4 . The lateral growth was achieved by applying an electric field of ~1 V/cm between the two cathodes while the average voltage between an anode (i.e. copper electrode) and each cathode was of 1.25 V. The large voltage difference between the anode and the cathodes resulted in concurrent reduction of copper at the cathodes and evolution of hydrogen (i.e., HEA).

As a part of this research the effect of H_2SO_4 and CuSO_4 concentrations on the lateral growth speed was studied. Incrementing the acid concentration in the aqueous solution to 1.5 M (H_2SO_4) and using the HEA electroplating process at room temperature showed a direct relation in the acceleration of the deposition rate reaching a speed of 110 $\mu\text{m/s}$. Despite the porous

structure, the HEA electroplated copper showed a similar conductivity as solid copper and a remarkable mechanical strength suitable for use as interconnects on an electronic circuit.

In HEA, concurrent to the copper reduction, hydrogen bubbles are generated at the cathode resulting in a porous copper layer. However, the application of constant voltage does not allow bubbles to leave the surface of the electroplated electrode resulting in a non-uniform copper growth which in turn results on an unpredictable micro and nanostructures. To address the problem, we have studied the effect of superimposing a low frequency triangle shape AC to the DC potential to allow the hydrogen bubbles leaving the surface. The results clearly show that by controlling the AC and DC voltages around 100 mHz AC, a fast copper layer with fern shape nano structure can be achieved.

Further, the feasibility of adopting HEA electroplating method for patterning an electronic circuit on fabrics has been tested for copper deposition on a few different samples of fabrics. To provide the conductive path for the electroplating, first, the desired pattern was applied as a template on the fabric using a conductive ink including multiwalled carbon nanotubes (MWNTs). It was found that the type of the fabric affects the copper growth rate. The fastest copper growth rate was achieved on 1000 Denier Coated Cordura Nylon sample, while 100% Virgin Vinyl sample showed the slowest growth rate. Further study of the morphologies using the scanning electron microscopy (SEM) technique showed that the material being used as substrate has a direct relationship with the morphology of the electroplated copper as well as the scan rate and the potential range being applied.

The observed low resistance of the electroplated copper is a promising sign that HEA electroplating can be used for rapid copper deposition on various substrates. The produced hydrogen bubbles from the HEA electroplating formed a porous structure while the copper

growing was taking place with a speed rate a few orders of magnitude higher than the growth speed in the conventional copper electroplating. The presented results in this dissertation verify the feasibility of using the HEA electroplating as a viable method for making copper-based circuit layouts directly on fabrics.

Chapter 1: Introduction

Copper has been used as one of many materials for plating over non-metallic and metallic surfaces. It has a broad range of applications in many industries such as in the manufacturing of electronic components, automobile, biomedical and aerospace. Over decades, copper has been a key material for the development of integrated circuits in cellphones, computer, and other electronic devices thanks to its high conductivity and processability for its integration to different substrates. To assure that the properties of copper are being used to the maximum, the electrochemical technique known as electroplating has been used in industry. The usage of this technique for the development of devices and electronics is seen as responsible for the increasing number and widening types of applications. This have allowed an increment of economy and convenience by the prevention of corrosion, and by permitting a significant increment of the electrical conductivity.

Electrodeposition of metals is the most cost-effective way to achieve deposition commonly used in the electronics manufacturing industry. It is primarily used to achieve high density interconnects in PCBs playing an important role in the electronic industry. It also provides a high quality of the deposits requiring relatively inexpensive equipment [1]–[5]. Metallization of substrates by copper electrodeposition enhances the electric conductivity of their surfaces potentially leading to an improvement of their electron transfer properties and a direct impact to the growth rate of the metal being plated [6].

Electroplating, or commonly known as electrodeposition, is a process for making a thin-film coating of a metal on a conductive object via passing a DC current in an electrochemical cell

in which the target object is used as the working electrode. The primary use of electroplating is to change physical properties, to increase wear resistance, to increase the thickness, or to give corrosion protection to the object. The growth of the market can be attributed to the rising adoption of electroplating across various industry such as the automotive industry and aerospace and defense among others [7][8]. Through the years, this technique has been modified and improved, opening new venues for developing new copper electroplating approaches used in the production of many electrical devices and circuit interconnect for fabrication PCBs [5][9][10].

Fast and lateral copper growth can open ways for depositing copper on various substrates to build electronic circuits for wearable and flexible electronics providing an incredible speed of growing metals compared to the conventional galvanostatic electroplating [5]. While the electronic circuit manufacturing is well developed for fabricating circuits on solid and flat PCBs, the application of electroplating for the production of flexible and wearable electronics has been largely ignored, mainly due to the compact and rigid structure of deposited copper and the low deposition rate through the conventional galvanostatic (i.e. using constant DC current) method but with the advantages in the development of wearable and flexible electronics, there is an increasing demand for lightweight, flexible, and wearable human and environmental monitoring systems with countless applications [5].

The wearable electronics market is predicted to develop from its present-day value of USD 40 billion to a full-size price of USD 160 billion through 2026 [11]. Over the years, flexible devices and wearable systems have gained significant attention in the scientific and commercial field. Yet, a challenge is in the development and integration of electrodes and interconnects at any desired shape and size with enough flexibility and electrical conductivity suitable for flexible and wearable electronics [12]. With the developing technologies at a worldwide level electronic textile are

emerging cutting across traditional industrial procedures. The development of flexible materials is essential for wearable electronics because of their unique chemical, electrical, and mechanical properties. Replacing relatively poor mechanical flexibility and stretchability such that they can be conformally attached onto the human body for clothing, communication, healthcare monitoring, military, sensors, among others playing a key role among various technologies. Along with advantages in the development of wearable and flexible electronics, there is an increasing demand for lightweight, flexible, and wearable human and environmental monitoring systems with countless applications [13]. Developing e-textiles demands a fabrication method to integrate electronic components and circuits into fabric structures with the interconnect conductivity as high as that in copper ($\sim 6 \times 10^7$ S/m) [14] and a printing method with the feature size less than 1 mm to be compatible with the packaging of surface mount devices (SMDs). In addition, the adaptation of the current available devices and attachment-based wearables into integrated technology may involve a significant size reduction while retaining their functional capabilities [13].

Among different technologies and approaches, patterning a conductive template (i.e. circuit layout) on fabrics by copper electrodeposition can lead to the development of different wearable and flexible electronics [15]. Carbon materials have recently brought attention due to its significant properties which have allowed us to use the multiwall carbon nanotubes (MWCNTs) as electrode over a variety of fabrics employing the novel technique called hydrogen evolution assisted (HEA) electroplating, to enhance the lateral deposition of copper and its properties leading to the development of useful wearable electronics with the goal of overcome the existing challenges and create future opportunities [16][17]. This technique can electroplate the surface of a conductive pattern with a growth rate of at least four orders of magnitude faster than the conventional galvanostatic electroplating speed and produces nanostructures for embedding the printed structure

to the fabric fibers. Surface modification of textiles with desired functionalities can be engineered by a considerable number of techniques ranging from traditional treatments to multifunctional approaches. Textiles, in fact, offer a challenging platform for functional modifications to meet additional strategic requirements for a large variety of applications [17].

In this dissertation, chapter 1 is dedicated to the introduction. Background and the literature review of the copper electrodeposition technique by the employment of different methods and wearable electronics are discussed in Chapter 2. Chapter 3 reflects our experimental studies on low temperature soldering with hydrogen assisted copper electroplating and the integration of surface mount components to printed circuit boards. Chapter 4 discusses the impact of CuSO_4 and H_2SO_4 concentrations on lateral growth of hydrogen evolution assisted copper electroplating and its relationship with the growth rate of copper. The copper electrodeposition assisted by hydrogen evolution has been employed in different substrates such as fabrics for the development of wearable electronics using a low temperature and low-cost procedure as discussed in Chapter 6. Chapter 7 includes the advantages in performing copper electroplated for the development of metallic tracks over different types of fabrics by using hydrogen evolution assisted electroplating. The conclusion of the dissertation and suggestions for future work are discussed in Chapter 8.

Chapter 2: Background

An electrochemical cell can transform chemical reactions into electrical energy or vice versa depending on the type of electrochemical cell being employed. There are two types of electrochemical cells known as galvanic or voltaic cell and electrolytic cell as shown in table 1. Both cells are composed of electrodes known as cathode and anode and an electrolyte to complete the electrochemical cell.

Table 1. Types of Electrochemical cells

Electrochemical Cells	
<i>Galvanic Cell (Voltaic Cell)</i>	<i>Electrolytic Cell</i>
The redox reactions take place spontaneously.	The redox reactions are non-spontaneous needing a DC or AC power source to fulfill the reaction.
Chemical energy is spontaneously transformed into electrical energy.	Electrical energy is transformed into chemical energy.

Due to the limitation imposed by the ions mass transfer in the electrochemical cell, the copper growth rate is usually slow in a galvanostatic deposition mode using a constant DC current source. Instead of controlling the process with a constant current, a constant DC voltage or AC voltage can be applied between the anode and cathode (i.e. potentiostat mode). However, increasing the potential to higher than 1.23 V leads to the release of hydrogen bubbles (i.e., HEA) at the working electrode. Nebojsa et al., have found that during the electrochemical decomposition

of a substance through the passage of an electrical current known as water electrolysis, the hydrogen evolution assists convection of copper ions toward the cathode at which the hydrogen is evolved and positively charged ions migrate towards the cathode, resulting in much faster rate of the copper deposition than the galvanostatic mode, generating a porous copper layer [15][18]. Regarding the direct effect of hydrogen and copper ions, the electrolyte concentration affects the nanostructure of the electroplated layer leading to the formation of various shapes and density of cauliflower-like, dendritic and honeycomb-like structure [5][19].

If an electric field is applied across an electrolyte solution by the usage of two electrodes as shown in Figure 1, in this case two working electrodes to achieve later copper electrodeposition and applying a DC or AC potential difference it will encourage motion of the charged ions in the electric field between electrodes immersed in solution allowing the flow of electrical current through the electrolyte and towards the working electrodes [18].

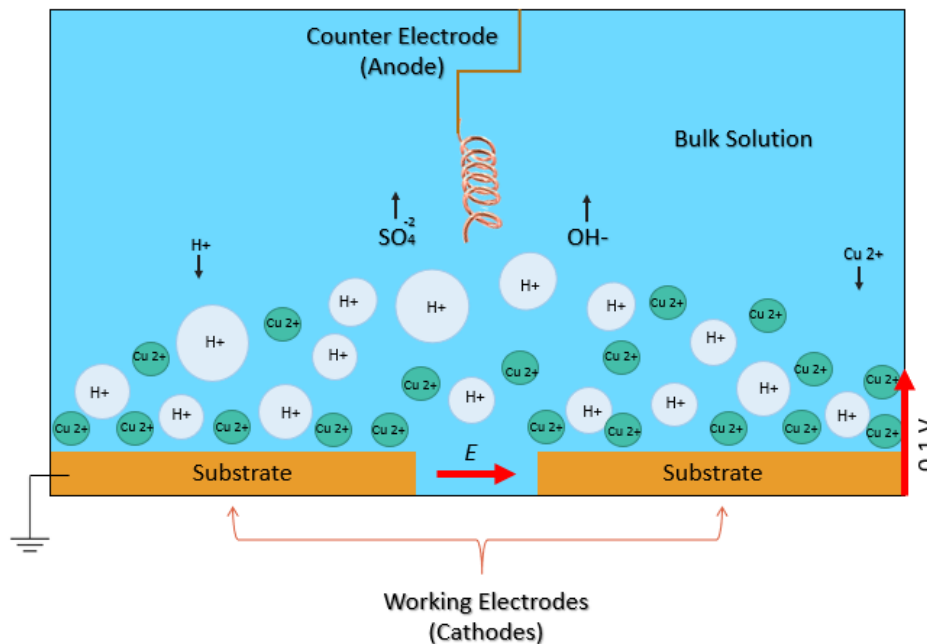


Figure 1. Schematic diagram of the electrochemical cell employing the redox reaction and hydrogen evolution assisted electroplating.

There are three essential mechanisms that have a direct impact on the copper electrodeposition: diffusion, migration and convection. In the conventional galvanostatic method the diffusion is the one that limits the growth rate of the copper after reaching equilibrium from the movement of molecules from a high concentration to a low concentration area. This can be seen in the Nernst-Planck Equation where the flow of ions is due to the spatial difference in concentration and the migration of ions due to the spontaneous reaction, lacking the convection mechanism. It is important to emphasize that many times the electrolyte that contains the electrodes is stationary, meaning that there is no convection by hydrodynamic transport. The diffusion, migration and convection are related by the Nernst-Planck Equation [18]:

$$J_i(x) = -D_i \frac{\partial C_i(x)}{\partial x} + \frac{-Z_i F}{RT} D_i C_i \frac{\partial \phi(x)}{\partial x} + C_i v(x) \quad (1)$$

where $J_i(x)$ is the overall flux of species i , D_i represents the diffusion coefficient having a negative sign meaning that molecules always diffuse from an area of higher concentration to an area of lower concentration, $\frac{\partial C_i(x)}{\partial x}$ represents the concentration gradient, Z_i represents the valence of i ions, F represents the Faraday constant ($\sim 96485 \text{ C mol}^{-1}$), R the universal gas constant ($8.314 \text{ J mol}^{-1} \text{ K}^{-1}$), T represents temperature, C_i represents the concentration of i , $\frac{\partial \phi(x)}{\partial x}$ electric potential gradient, $v(x)$ velocity at which the specie i moves.

Potentially, the HEA electroplating can address the need for fast copper deposition by assisting the motion of copper ions beyond the limited diffusion rate by convection and migration[20]–[22]. After electrolysis is reached, hydrogen evolution assists convection of copper ions toward the cathode, resulting in much faster rate of the copper deposition than the galvanostatic mode [5].

The proposed HEA electroplating of copper is a promising approach for developing highly conductive patterns over fabrics, but the process requires having a conductive template on the target substrate. Integration of copper electrodeposition assisted by hydrogen evolution technique with the addition of fabrics will allow the development of smart wearable electronics by the integration of electronic circuits into fabrics opening new venues toward new techniques and applications in electronics, medicine, aerospace, and military approaches.

2.1 Literature Review

The conventional electroplating process aims to control the electrodeposition process to maintain a constant deposition rate for achieving a compact and uniform layer of coating. Any factor that disturbs the process affects directly on the quality of the electroplated layer. Significant efforts have been done to control the shape and size of produced nanostructures when the electroplating process is intentionally disturbed. The disturbance can be generated by the application of an overpotential (DC or AC), magnetic field, pulsating current, reversing current or galvanostatic (DC regime) as electroplating methods (Table 2) [23].

Table 2. Electrodeposition techniques

Method	Uniformity	Time	References
Galvanostatic (DC regime)	✓	✗	[23]
Pulsating Current	✓	✗	[23]–[35]
Reversing Current	✓	✗	[23],[24] [28],[36]–[38]
Magnetic Field	✗	✗	[39][40]
DC & AC Overpotential (potentiostat)	✓	✓	[5][41]

Pulse electrodeposition (PED) is divided in two significant areas pulse reverse current (PRC) and pulsed current (PC), both areas have brought many advantages at a manufacturing level but with advantages, there is always a disadvantage that needs to be strongly studied [24]. The electroplating of pulse reverse current (PRC) is an electrochemical process technique where the application of the current is alternated between a cathodic current (forward pulse) and an anodic current (reverse pulse) during the electroplating process. Reversed pulse plating may offer several advantages to on-off pulse plating such as reducing brightener decomposition and allowing a reduction in defects of the electroplated metal layer [28][36]. Nebojsa and his group have done extensive research on studying copper nanostructures grown via the HEA electroplating process [29], [42], [43]. In one of their works published in 2012, they have shown that the reversible current (RC) regime is superior in the production of open porous structures in comparison with the pulsating current and the galvanostatic regimes [23].

The reverse pulse technology has demonstrated to improve specific properties of the deposition such as hardness and to reduce the total time of process decreasing the copper consumption significantly. Today, pulse reverse (PR) plating is widely used in printed circuit board (PCB) manufacturing and by combining hydrogen evolution assisted electrodeposition with pulse-reverse electrodeposition a high surface area with highly porous metallic nanostructured can be obtained. As reported by Cherevko, et. al the convection created by the movement of the hydrogen bubbles increases the growth rate of copper and removes the dissolved copper ions from the diffusion layer [37][38]. Both the morphology and the hydrogen evolution have significant impact on porosity. The application of RC regime led to redistribution of evolved hydrogen increasing the compactness of the honeycomb-like structure obtained by RC. Even though the RC was successful

in the formation of a honeycomb-like structure by the direct interaction of HEA electroplating over the substrate's surface, the deposition time is still a problem.

As studied by Popov, et. al the pulsed current (PC) plating offers a smoother and less porous deposits compared to conventional direct current plating DC producing a significant change in the morphology of the electrodeposits, which may also improve other mechanical and electrical properties [28],[37],[25]–[27], [30]–[35]. With the pulsating current and DC regime the appearance of dish-like holes was visible. It was found that both on– off pulse plating and reverse pulse plating can result in lower porosity[28].

The process of copper growth by copper magneto-electrodeposition (MED) has a duration of 20 minutes [39]. A similar work has been conducted by Beatriz, et. al where the effect of hydrogen evolution is being studied and how the magnetic field simultaneously increases the rate of hydrogen evolution and modifies the hydrogen bubble size and dislodge them as they form [40]. A reduction in the size of the bubbles was obtained by reducing the magnetic field applied. An irregular copper growth was observed based on a mixture of holes, dendrite, and cauliflower-like structure, not providing any uniformed morphological structure. As shown by Sudibyo et al., it has been found that different strengths of magnetic field will affect the growth pattern and the morphology of the copper being deposited, not allowing them to properly cover the surface of the substrate [39]. They have found that dendritic structures grow larger and more compact as the concentration of CuSO_4 increases, which inhibits more copper from deposition within the dendrites. An increment in CuSO_4 in the electrolyte the copper deposits start to increase in a nonlinear fashion way not being able to control the pattern.

However, in the galvanostatic technique the instrument controls the cell current rather than the cell voltage, with the application of this direct current electroplating the problem manufacturers face is in controlling the amount of copper inside the holes. As the number of copper layers needed for the deposition increase there is also an increment in the entire plating time which will take two to three hours longer to complete.

As we have studied, as well as Nebojsa, et. al and Heon-Cheol, et. al, the application of an over potential higher than 1.23 V leads to the release of hydrogen bubbles (i.e., HEA) at the working electrode that generates a porous copper layer with much faster growth rate than the conventional galvanostatic electroplating method allowing the current to flow between the working electrode and the counter electrode to complete the cell circuit [5][41]. It has been shown that hydrogen bubbles play a crucial role in the formation of porous structures leading to a well mechanical supported structure and the impact that the concentration of acid has in the deposition of copper. Although significant works have been done for controlling the morphology of HEA electroplated copper, there is a gap of knowledge on how to employ the HEA electroplating method for metallization of conductive fabrics to develop a manufacturing method for wearable electronics. Recently we have employed the usage of the potentiostat by the application of an AC overpotential to increment the deposition of copper over printed circuit boards and fabrics with the main goal of allowing the hydrogen bubbles to be released from the surface allowing more copper to be deposited as metal over the cathode.

Chapter 3: Low Temperature Soldering Surface-Mount Electronic Components with Hydrogen Assisted Copper Electroplating¹

3.1 Introduction

Technology is always in the need of improvement to develop new devices and enhance procedures. With the recent development in 3D printings, fast and in-house prototyping of mechanical structures has become feasible [44]. However, electronic circuit's prototyping is still required advanced facilities for lithography of PCBs and automated pick-and-place machines for soldering surface mount electronic components. Several approaches have been demonstrated before for using a printing technique for prototyping electronic circuits [45][46]. The most common method is the inkjet printing for making a PCB using conductive inks made of silver or copper nanoparticles [47]. After printing, the substrate must be heated up to remove the solvents and melt the nanoparticles to form continuous conductive tracks. The approach has several technical challenges which limit its application to only simple circuits. For instance, the substrate must be flat and smooth and being made of materials with high melting temperatures. Due to the low melting temperature of the plastics, conventional soldering method using a soldering iron is not practical. Hence, conductive pastes have been the only option which is not as reliable as conventional soldering materials, due to their lower conductivity and adhesion. To overcome the problems for integrating electronics to a 3D printed structure we have studied the feasibility of using copper electroplating for soldering electronic components to conductive tracks at room

¹ This chapter was published before in MRS Advances (Sabrina M Rosa-Ortiz, Kishore Kumar Kadari, Arash Takshi, "Low temperature soldering surface-mount electronic components with hydrogen assisted copper electroplating", MRS Advances (2018), 3, 18, 963-968). Permission is included in Appendix I.

temperature using printed circuit boards (PCBs). Although the method is potentially practical, the low deposition rate of copper is a major drawback. In this work we are demonstrating the hydrogen evolution assisted (HEA) electroplating [15] as a rapid method of growing copper for soldering surface-mount electronic elements, suitable for electrodes in many electrochemical devices, such as fuel cells, batteries, and chemical sensors [9]. The results show a promising approach for further development of the method for low temperature soldering of electronic components.

3.2 Experimental

The electrolyte for electroplating was prepared by making a solution of 0.4 M of CuSO_4 (from Sigma) and 1.3 M of H_2SO_4 (from Sigma) in deionized (DI) water. For the experiments on a PCB board, first the pattern shown in Figure 2 was applied on the copper side of the PCB using a permanent marker. The copper pattern was developed by etching the exposed copper in a ferric chloride solution (from MG Chemicals). The two tracks with 1 mm gap were used to mimic a gap between the terminal of an electronic component and the circuit layout. The objective was to bridge the gap using the electroplating method. An O-ring was placed over the gap between the two tracks to build an electroplating bath. For testing the copper bridging across the gap, the tracks were used as cathode 1 and 2, each connected to a voltage source via the pads. Also, each track was covered with the permanent marker except for a small part of the copper near the gap (see Figure 1). The larger copper pad (not covered by any layer) near the gap was used as the shared anode (the source of copper for electroplating). For the HEA soldering experiment, a surface-mount LED was placed across the gap and only one cathode was used. The other terminal of LED was soldered to the second track using a soldering iron. A microscope camera was set above the sample to record the electroplating process. The O-ring area was filled with the electrolyte, and a Keithley 2602 dual channel source-measurement unit was used as the voltage sources and data logging system. The

quality of the electroplated area was tested by resistance measurement and scanning electron microscopy (SEM) methods after the electroplating process.

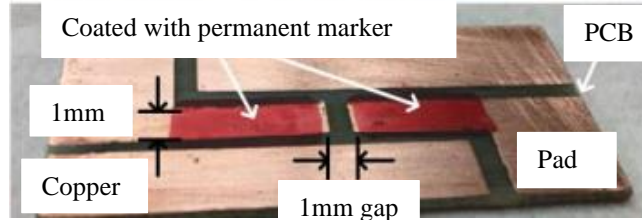


Figure 2. PCB sample was used to study HEA copper electroplating across the gap.

3.3 Results and Discussion

Using the patterned PCB in Figure 2, the electrochemical deposition was carried out by applying 0 V to the anode and -0.5 V to each cathode. While the recorded current showed an ongoing electroplating, the video recorded images did not show any visible change on the patterned copper even after several minutes of electroplating. The observation was in a good agreement with the theory of the electroplating. The thickness of the electroplating layer, d , is a function of time, t , and the current density, J , through the Faraday equation [8]:

$$d = \frac{JM_w}{nF\rho} t \quad (2)$$

where M_w is the atomic weight of copper (63.5 g/mol), F is the Faraday constant (~ 96485 C/mol), n is the change in the oxidation state ($n=2$ for Cu^{2+} to Cu), and ρ is the copper density (8.63 g/cm³). In the equation, the speed of growing copper (electroplating rate) can be calculated from $J.M_w/n.F.\rho$. A typical current density of 20 mA/cm² implies ~ 7.6 nm/s rate [9]. With such a rate, no visible change is expected even after several minutes of electroplating.

To increase the electrodeposition speed, first, we tested the electroplating process at higher voltages up to ~ 0.8 V between the anode and each cathode. Although the current density can be enhanced at the elevated voltages, the deposition rate was increased by a few folds, still not making

any visible change. However, for voltages above 1.0 V we observed hydrogen bubble release near the cathode due to the concurrent water hydrolysis and copper deposition. As shown in Figure 3, for a case with -1.2V to cathode 1 and -1.1V to cathode 2 (with respect to the common anode at 0V), the hydrogen bubbles were released from the electroplated area. In many conventional applications such as jewelry electroplating, hydrogen evolution should be avoided (by limiting the voltage) for depositing a compact copper layer. However, we have found that the release of hydrogen bubbles can assist the electroplating process; hence, dramatically increasing the copper deposition rate. In fact, as shown in Figure 3, the hydrogen evolution assisted (HEA) process resulted in a rapid growth of copper across the gap reaching a speed of $\sim 33 \mu\text{m/s}$. The high-speed growth came with the cost of losing the compact structure and depositing a porous structure instead. The dramatic increase in the electroplating rate can be explained via Equation 2. The density, ρ , of a porous structure can be significantly lower than that in a compact layer, resulting in an increase of the electroplating rate ($J.M_w/n.F.\rho$) even for a limited current density.

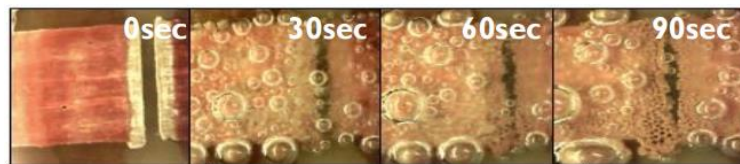


Figure 3. Images of the HEA electroplating across a 1 mm gap on a PCB sample.

The graph in Figure 4 shows the recorded current density during the electrodeposition. The large fluctuation in the current is due to frequent hydrogen bubble release. Application of a voltage slightly different than cathode 1 to cathode 2 generated a lateral electric field across the gap which increased the lateral electroplating speed. The resistance across the bridged electroplated area was measured to be 13.1Ω .

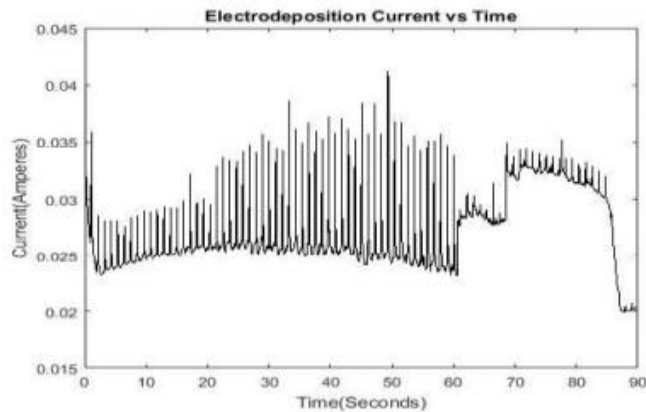


Figure 4. Current versus time during the electroplating of the PCB sample.

The concept of using HEA electroplating method for soldering an LED was also tested with a patterned PCB. Figure 5a shows the gap between the LED terminal and the copper track before the deposition. For the soldering process only one cathode (-1.2V) was used. Although the contact between the copper track and the LED terminal was made in about 30 s after starting the electroplating process, the experiment was conducted up to 55 s to make a reliable contact. The electroplated copper across the gap is shown in Figure 5b. To study the effect of bubbles and the electrolyte on the functionality of the device, the LED was tested after removing the electrolyte (Figure 5c and 5d).

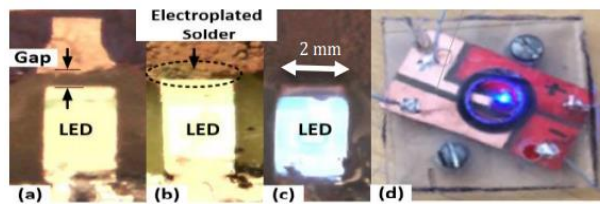


Figure 5. Images of the low temperature soldering of a surface mount LED (a) before and (b) after the HEA copper electroplating. (c) Powered LED. Confirming that the HEA process did not damage the LED. (d) Testing the HEA soldered LED in the electroplating setup after removing the electrolyte

3.4 Conclusion

The electrodeposition conducted by single cathode terminal configuration at low voltages had a slow copper growth rate not suitable for printing a circuit layout or soldering. At high voltages, the hydrogen evolution effect was observed during the electrodeposition resulting in a dramatic increase of copper growth rate in PCB samples. The high growth rate was achieved due to the growth of more porous copper structure (because of the hydrogen bubbles) instead of a compact structure. The significant advantage of the HEA electroplating method is in its fast growth rate that can be used in the future for developing a copper printing method. Printing copper will facilitate electronic circuit prototyping and enable soldering the components while printing copper.

Chapter 4: Study the Impact of CuSO₄ and H₂SO₄ Concentrations on Lateral Growth of Hydrogen Evolution Assisted Copper Electroplating²

4.1 Introduction

Electrodeposition plays an important role in the electronic industry representing a major advantage over other conventional methods, providing a high quality of the deposits requiring relatively inexpensive equipment [3] [4]. Through the years, this technique has been modified and improved, opening new venues for developing new copper electroplating approaches used in the production of many electrical devices and circuits. Compared to other metals, copper has applications as an improved interconnect material for fabrication of printed circuit boards (PCBs), which have diminished in size along with the miniaturization and high efficiency of electronic devices [9] [10]. Yet, application of electroplating for production of flexible and wearable electronics has been largely ignored, mainly due to the compact and rigid structure of deposited copper and the low deposition rate through the conventional galvanostatic (i.e., using constant DC current) method. Potentially, the hydrogen evolution assisted (HEA) electroplating can address the shortcomings by producing porous structure of copper and high rate of the metal growth [20] [21]. This work has focused on studying the effect of electrolyte concentration on the morphology and lateral growth rate of copper using the HEA electroplating method. The results are providing a guideline for further development of HEA lateral electroplating method to be used for patterning

² This chapter was published before in the Journal of Applied Electrochemistry (Sabrina M Rosa-Ortiz, Fatemeh Khorramshahi, Arash Takshi, “Study the impact of CuSO₄ and H₂SO₄ concentrations on lateral growth of hydrogen evolution assisted copper electroplating”, Journal of Applied Electrochemistry (2019), 49,12, 1203-1210). Permission is included in Appendix I.

copper on fabric substrates [48]. The mechanism of conventional galvanostatic copper electroplating with one anode and one cathode is based on two electrochemical reactions taking place at both electrodes in an electrochemical cell containing an electrolyte (typically is an aqueous solution of CuSO_4 and H_2SO_4 [49]). Oxidation starts taking place at the anode (counter electrode) where copper metal is oxidized to copper ions ($\text{Cu} \rightarrow \text{Cu}^{2+} + 2\text{e}^-$). At the working electrodes, reduction of the ions ($\text{Cu}^{2+} + 2\text{e}^- \rightarrow \text{Cu}$) occurs to form a solid metal coating. Due to the limitation imposed by the ions mass transfer in the electrochemical cell, the copper growth rate is usually slow in a galvanostatic deposition mode. Instead of controlling the process with a constant current, a constant DC voltage can be applied between the anode and cathode (i.e., potentiostat mode). However, increasing the over-potential to higher than 1.23 V leads to the release of hydrogen bubbles (i.e., HEA) at the working electrode that generates a porous copper layer with much faster growth rate than the conventional galvanostatic electroplating method. HEA electroplating has been studied extensively by Nikolić et al. [15]. They have found that during water electrolysis, the hydrogen evolution assists convection of copper ions toward the cathode, resulting in much faster rate of the copper deposition than the galvanostatic mode. As the result of the co-reduction of Cu^{2+} and H^+ ions, the process produces an open and porous structure of copper that can be employed in a generally wide range of applications such as fuel cells, batteries, and sensors [15], [41], [50]–[53]. Regarding the direct effect of hydrogen and copper ions, the electrolyte concentration affects the nanostructure of the electroplated layer leading to the formation of various shapes and density of cauliflower-like and dendritic structures [19]. The results from previous studies are showing the potential of the HEA copper electroplating as a method for a fast deposition rate [16]. However, to the best of our knowledge, the lateral growth of copper using the HEA method has not been studied before. Based on that, our research is focused on adapting the process for lateral growth of

copper to develop a printing method. In this work, we have studied the effect of ions concentration on the lateral growth rate and quality of the HEA electroplated copper. Fast lateral growth can open ways for printing copper on various substrates to build electronic circuits for wearable and flexible electronics providing an incredible speed of growing metals compared to the conventional galvanostatic electroplating. For the lateral growth, the electrochemical cell was designed with two cathodes on the same substrate, while an electric field of 0.1 V mm^{-1} was established between them to enhance the predominant growth.

4.2 Experimental

For studying the lateral growth of copper, the cathode electrodes with a width of 3 mm and a gap of ~ 1 mm were patterned on a piece of flame retardant-4 printed circuit board (FR-4 PCB) with measures of 5×2.5 cm. As shown in Figure 5, a permanent marker was used to make a mask, thereafter the unmasked areas were etched by ferric chloride (MG Chemicals). The large copper pads were used as the anode. To study copper growth near the gap, both working electrodes were covered with a red permanent marker, leaving an uncovered surface area of 0.23 cm^2 at the one end of each electrode near the gap, for the copper deposition to take place. The experiments were designed by making a small electrochemical cell around the gap on the PCB using an O-ring with the diameter of 2.54 cm, to hold the electrolyte. In this work, we studied the HEA lateral copper growth rate using aqueous based electrolytes containing various concentrations of CuSO_4 and H_2SO_4 (both from Sigma-Aldrich). In a set of experiments, electrolytes with constant concentration of CuSO_4 (0.15 M) and H_2SO_4 at different concentrations of 0.125 M, 0.25 M, 0.5 M, 1.0 M, 1.5 M, 2.0 M, and 2.5 M were made. To study the effect of CuSO_4 , the electrolytes were prepared with 0.1 M, 0.15 M, 0.2 M, and 0.25 M concentration of cupric sulfate using 1.0 M and 1.5 M of H_2SO_4 for each CuSO_4 concentration. In each experiment, 2 mL of the electrolyte

was used inside the O-ring area to make the electrochemical cell for the experiment. Electrodeposition was carried out using a Keithley 2602A SMU connected to a computer. Using Test Script Builder program, a simple code was developed to collect the electrodeposition current data and the current between the two cathodes. A digital camera microscope video recorded the electrodeposition process. To establish a voltage difference between the two cathodes, -1.3 V was applied to one of the cathodes and -1.2 V to the other cathode. As it can be observed in Figure 6, another copper pad was used as the anode contact biased at 0 V. For the soldering purpose, only one probe was used to grow the copper at the gap between the copper traces and a surface mount device (SMD) light emitting diode (LED). The applied voltage to the cathode (copper trace) was -1.3 V with respect to the anode. After conducting the experiment, the electrolyte was removed using a pipette and the samples were rinsed with DI water. The samples were left for 24 hours at room temperature before testing their morphologies using a scanning electron microscope (SEM) (Hitachi S-800) at 25.0 kV. To estimate the porosity level in the HEA electroplated layer, cyclic voltammetry (CV) experiment was conducted in a three-probe arrangement using a VersaStat 4.0 potentiostat. For the experiment, an Ag/AgCl and a Pt wire were used as the reference and counter electrodes. A 1.0 M Tris-buffer at pH of 8.0 (HCl) was used as the electrolyte in the CV measurement.

As an example, to show the effect of hydrogen evolution during the HEA process, pictures were taken from a sample before, during, and after the electroplating for the experiment with the electrolyte of 1.0 M H_2SO_4 and 0.15 M CuSO_4 (Figure 7). Figure 7a shows the 1 mm gap between the two copper traces which were used as the working electrodes in the electrochemical cell. Once the voltage difference was applied to the electrodes, the release of the bubbles was observed

(Figure 7b). The further the hydrogen bubbles from the gap between the two working electrodes the larger the diameter (>2 mm) based on the coalescence between them.

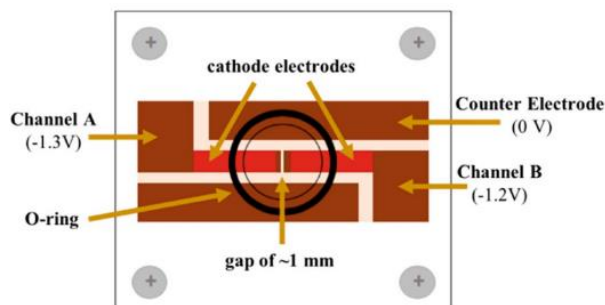


Figure 6. Schematic of the patterned electrodes on a PCB and the O-ring area for the electrochemical cell. The cathodes were connected to channels A and B of a Keithley instrument while one of the big pads was used as the common anode (counter electrode)

4.3 Results and Discussion

This indicated that the water electrolysis was taking place, incrementing the release of bubbles with respect of time. During electrolysis, hydrogen evolved at the cathode caused the structure of the electroplated layer to be more porous due to the attachment of hydrogen bubbles and agglomerate of copper grains between them leading to formation of a variety of morphologies of copper deposits while remaining similar conductivity in the deposited copper area [16], [29], [42], [43]. The rate of hydrogen release was significantly higher around the electrode biased at -1.3 V due to the higher applied voltage in comparison to the other electrode (biased at -1.2 V). Also, the copper growth rate was higher at the electrode biased at -1.3 V. For the electrolyte containing 1.0 M H_2SO_4 and 0.15 M CuSO_4 , after 58.8 s the copper bridged the gap between the two electrodes. Continuing the process to 67.8 s a stronger joint was established between the two cathodes (Figure 7c).

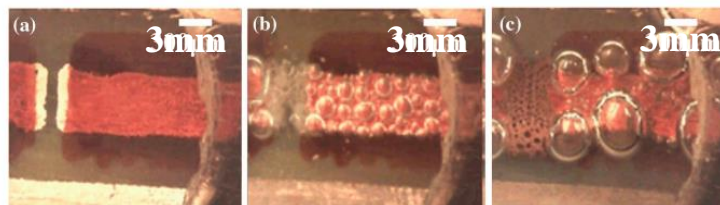


Figure 7. Images of copper deposition with a magnification of $21\times$ using hydrogen evolution assisted (HEA) electroplating for 0.15 M CuSO_4 in 1.0 M H_2SO_4 : a) before, b) during (30 s after starting), and c) after electroplating (67.8 s electroplating duration)

Although Figure 7 shows pictures of only one sample, similar behavior of generating bubbles during HEA and bridging the gap was observed in all samples tested with different electrolytes. After completion of the electrodeposition of copper when the anode was fully consumed, a contact resistance of 0.5Ω was measured for the electrolyte containing 1.0 M H_2SO_4 . Figure 8a shows the results of the current passing through channel A of the instrument (shown in Figure 6). The average current flowing through the anode while the deposition was taking place, was about 60 mA. The current value gradually increased through all the process, showing fluctuation in the current. The fluctuation in the current is believed to be due to the hydrogen bubbles generation and release at the surface of the electrode [16].

Based on the rapid diffusion of hydrogen ions to the cathode by the application of large voltages, a continuous growth process was allowed. The increase in the current value at 67.8 s confirmed the connection between two copper pads and the completion of the growth. The bridging was also detectable by measuring the current between the two working electrodes during the deposition process, using the Test Script Builder code on the computer. For this measurement (shown in Figure 8b), the current was measured when a 0.1 V was applied across the two electrodes while the growth potential was paused momentarily to take samples of the current between the two electrodes. The sudden jump in the current around 58.8 s again confirms the bridging. Knowing the size of the gap between the two cathodes (i.e., 1 mm) and the time of bridging the gap (from

the recorded videos), the lateral growth rate was estimated for the different samples that were tested. The lateral growth of HEA copper electroplating was found to be much faster than the copper growth without HEA electroplating. However, previous works by Nikolić et al. suggest that the concentration of acid has a direct influence on the morphology and the growth rate of HEA copper electroplating [20].

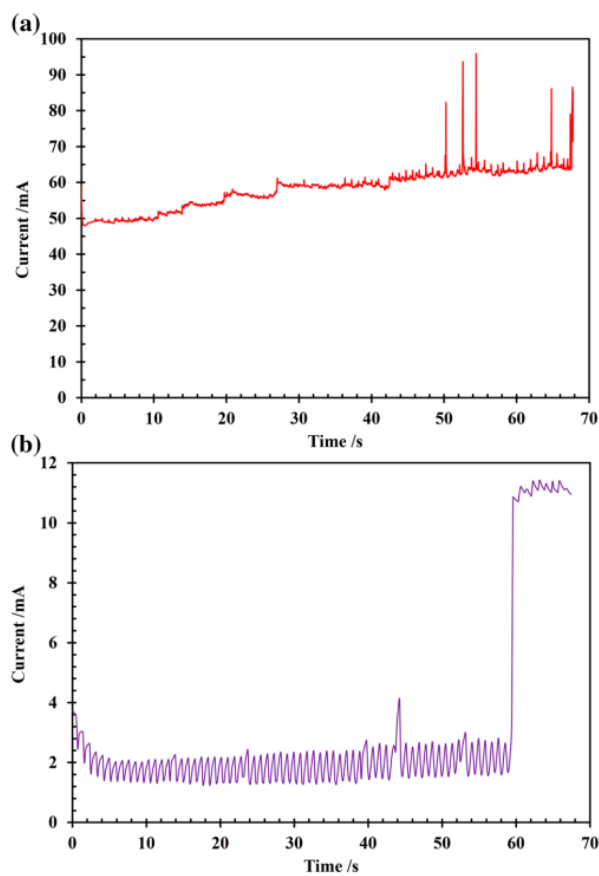


Figure 8. a) Electrodeposition current (A) vs. time (s) and b) current between the cathodes vs. time (s) for the electrolyte containing 0.15 M CuSO_4 and 1.0 M H_2SO_4

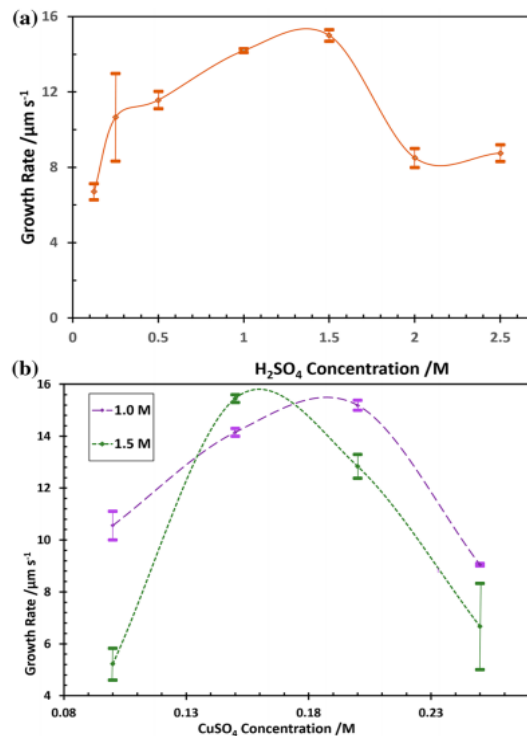


Figure 9. Lateral growth rate ($\mu\text{m s}^{-1}$) vs. acid concentrations (M) for 0.15 M CuSO_4 . b Lateral growth rate ($\mu\text{m s}^{-1}$) vs. copper sulfate concentration in 1.0 M H_2SO_4 and 1.5 M H_2SO_4

To find the effect of ions concentration on the lateral growth rate, similar electrodes were made and tested with different electrolytes. An estimation of the growth rate for a change in CuSO_4 and H_2SO_4 concentrations was made by dividing the distance between both working electrodes (~ 1 mm) and the time in which the junction between both electrodes was made. In the first round of the experiments, the concentration of CuSO_4 was kept constant at 0.15 M and electrolytes with 0.125 M, 0.25 M, 0.5 M, 1.0 M, 1.5 M, 2.0 M, and 2.5 M concentration of H_2SO_4 were tested. Figure 9a shows the estimated lateral growth rate versus the acid concentration. The error bar at each concentration shows the variation in the growth rate measured in different samples. At least two samples were tested for each concentration. Although there was a large difference between the maximum and minimum measured rate for samples at 0.25 M, the trend showed an increase in the growth rate up to 1.5 M acid concentration at which the growth rate reached $15.6 \mu\text{m s}^{-1}$.

The growth rate dropped to almost half of the value when the acid concentration was increased to 2.0 M, likely due to an intensive hydrogen evolution beyond 1.5 M leading to a strong decrement for current efficiency for the electrodeposition of copper. Since the two highest rates were achieved at 1.0 M and 1.5 M acid concentrations presenting growth rates of 15.38 and 15.6 $\mu\text{m s}^{-1}$, respectively, the second sets of experiments were carried out in which samples were tested with electrolytes containing acid H_2SO_4 at 1.0 and 1.5 M concentration and CuSO_4 concentration in the range of 0.1 and 0.25 M. The estimated lateral growth rates versus the CuSO_4 concentration are shown in Figure 9b with at least two samples for each concentration. For 1.5 M acid concentration the maximum growth rate was obtained when CuSO_4 concentration was 0.15 M, whereas in 1.0 M acid concentration the maximum was for the electrolyte with 0.2 M CuSO_4 . The effect of hydrogen bubbles released is reflected in the decrement of the growth rate after having reached the maximum for 0.15 and 0.20 M, respectively. The accumulation of bubbles on the surface leads to bubble agglomeration limiting the deposition of copper and therefore leading to a reduction in the growth rate. A difference of 35% in the growth rate was obtained between the lowest (0.125 M CuSO_4) and the fastest (0.25 M CuSO_4) growth rate reported for 1.0 M of H_2SO_4 in comparison with the 70% reported between lowest (0.1 M CuSO_4) and the fastest (0.15 M CuSO_4) growth rate reported for 1.5 M of H_2SO_4 . As shown in Figure 8a, the growth rate was the slowest at 0.125 M H_2SO_4 concentration, while for 1.0 M H_2SO_4 the growth rate was near to the highest value.

To understand the effect of the ions concentrations on the different growth rates, morphologies of copper deposits under the effect of the hydrogen evolution were studied through the SEM images for two samples grown in electrolytes with the acid concentration of 0.125 M and

1.0 M (CuSO_4 concentration of 0.15 M). As it can be seen in Figure 10, pores were surrounded by dendrites leading to a honeycomb-like structure [54].

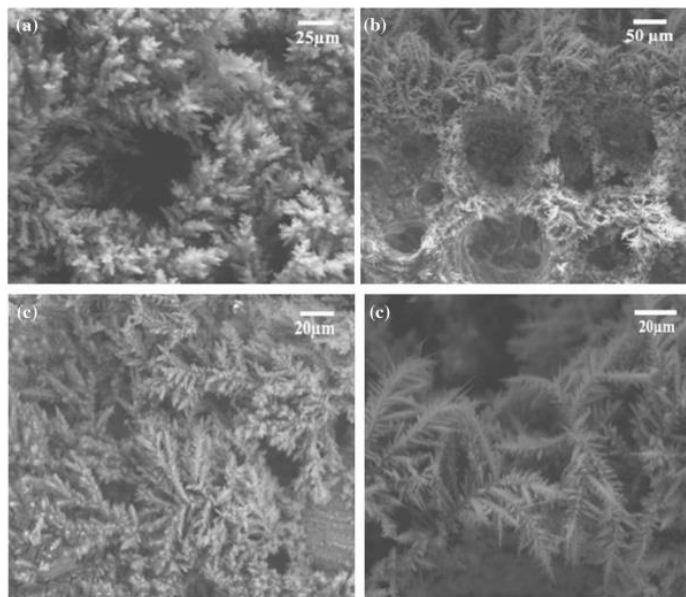


Figure 10. Holes made of copper deposits after hydrogen evolution assisted (HEA) electroplating for concentrations of 0.15 M CuSO_4 (a, c) in 0.125 M H_2SO_4 and (b, d) in 1.0 M H_2SO_4 . c and d are at 20 μm zooming scale showing the dendrite nanostructures

Comparing the size of the honeycomb structures in Figure 10a and 10b, higher concentration of the acid resulted in larger pore size. Also, the zoomed images on Figure 10c and d show the higher density of nano dendrites in the sample with the lower concentration of acid. As expected, the growth rate decreases with an increase in the density of the electroplated copper. This can be directly related to the size of the generated hydrogen bubbles at different acid concentrations. Due to the blockage of the surface at the locations that hydrogen bubbles were formed, copper deposition did not occur which generates a lower density structure [41].

The effect of the acid concentration on the nanostructure of HEA grown copper has been studied before [20]. According to Nikolić et al., as the concentration of acid increases, more stable structures with higher porosity in a honeycomb form are produced [20] [54]. The level of porosity

in the HEA grown copper was estimated with the CV method. In a three-probe configuration the voltage was scanned between -0.2 V and $+0.2$ V with a scan rate of 50 mV s $^{-1}$. The voltage range was limited to 0.2 V to avoid any redox reaction at the working electrode. As an example, the double-layer capacitance forming on the working electrode of the sample grown in the 0.15 M CuSO_4 and 1.0 M H_2SO_4 electrolyte was estimated to be 226 mF from the CV result (Figure 11a). Assuming the capacitance of a double layer to be ~ 0.2 F m $^{-2}$, the total surface area of the porous copper structure was estimated to be 1.13 m 2 indicating a very high level of porosity in the structure as it was confirmed by the SEM images [55]. More accurate porosity measurements using Brunauer–Emmett–Teller (BET) method is considered for future works. Also, the adhesion of the grown copper to the FR4 substrate was tested by the simple tape method [56]. In this method, the resistance of the HEA grown copper was measured with a handheld multimeter. A transparent office Scotch tape was placed over the grown copper. As shown in Figure 11b, the tape was removed at 90° angle and the resistance was measured afterward. The resistance of the sample was changed from 1.0 Ω (before the test) to 4.7 Ω (after the test). The optical microscope images in Figure 11b show the structural damage due to the peel-off process. Although the adhesion of the HEA grown copper is significantly lower than the cladded layer on the FR4 substrates, the nanostructures on the HEA electroplated layer can be used for growing copper on fabrics for development of wearable electronics with high adhesion to the fabric fibers.

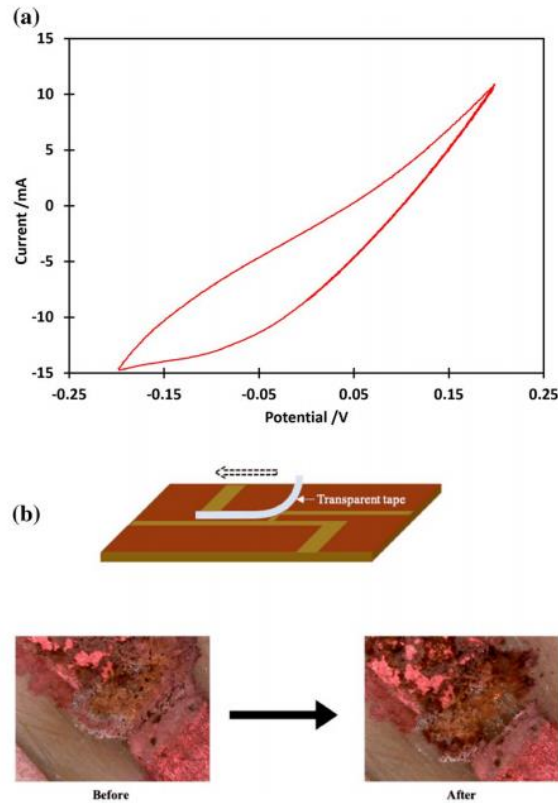


Figure 11. a) Cyclic voltammetry result for 0.15 M CuSO_4 and 1.0 M H_2SO_4 , b) Adhesion test of the sample using a transparent Scotch tape showing the pictures before and after the test. The dashed arrow shows the direction that the tape was removed.

Regarding the application of the HEA method for wearable electronics, an essential step for building circuits is to solder the components on the conductive tracks. In this work, we have tested the possibility of using HEA electroplating to solder a light emitting diode (LED) to the copper track on a patterned PCB. One terminal of the SMD LED was solder to one copper track. The other terminal of the LED was near the other copper track. To electrodeposit the copper to the free LED pin, only one channel was used between the copper track (cathode) and an anode in the solution. -1.3 V was applied to the cathode with respect to the anode for an electrolyte with 1.5 M H_2SO_4 . The soldering process was video recorded using the microscope camera on top of the junction. The deposition was carried out for 60 s, after its completion a porous structure was observed because of the agglomeration of hydrogen bubbles on the surface. Figure 12a and 12b

shows the LED before soldering and after. Figure 12c shows that after soldering, LED can be illuminated by applying a voltage to the copper tracks, verifying the soldered contact. Also, Figure 12d shows the growth current which was nearly 60 mA and constantly decreased with time. The decrease in the current was found to be due to the increase in the resistance of the cell because of fast consumption of the anode. The soldering resistance was found to be less than 2Ω after finishing the soldering process. Further study is required and planned to investigate the mechanical strength and shape of the nanostructures of the solder joints under various HEA electroplating conditions.

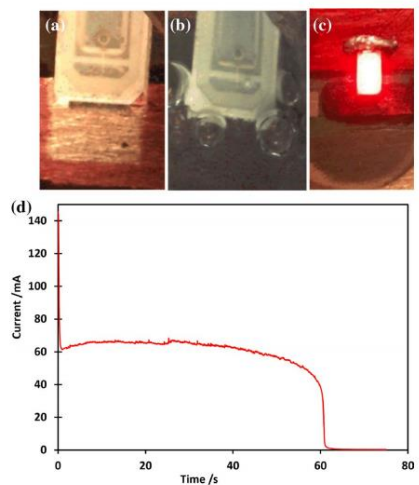


Figure 12. Light emitting diode (LED) configuration, a) LED over working electrode with gap for copper electrodeposition, b) copper junction between LED and working electrode after copper electrodeposition assisted by hydrogen evolution, c) light emitting diode (LED) configuration after applying a voltage using Keithley 2602A & d) electrochemical growth current during soldering the LED

Both lateral growth and soldering processes using HEA copper electroplating are promising for fabricating electronic circuits by electrochemically printing copper on a substrate and then soldering the components [57][58]. Particularly, the low temperature soldering method is suitable for fabricating wearable and flexible electronics, where the conventional soldering methods at high temperatures may damage the substrates. Conventional galvanostatic copper electroplating system

is based on applying a small overvoltage between the anode (i.e., copper electrode which can source soluble Cu^{2+} ions into the electrolyte) and a single cathode balancing the tendency of the metal ions to diffuse from the counter electrode to the electrolyte and to the cathode. For a uniform deposition of copper, it is recommended to apply a constant current density to the electroplating cell [22]. A typical current density of 20 mA cm^{-2} implies $\sim 7.6 \text{ nm s}^{-1}$ rate, which is three orders of magnitude smaller than the measured growth rate in our HEA electroplating method.

Considering the highest concentration of Cu^{2+} ions in this work (i.e., 0.25 M), it is unlikely to depolarize the cathode [22].

While a high concentration of Cu^{2+} may depolarize the cathode where reduction will take place and increase the growth rate, still the limitation in the deposition rate can be overcome (as applied in this work) by using a constant voltage source (instead of a current source) at such high voltages that in addition to copper reduction ($\text{Cu}^{2+} + 2\text{e}^- \rightarrow \text{Cu}$), hydrogen evolution would take place at the cathode ($2\text{H}^+ + 2\text{e}^- \rightarrow \text{H}_2$). Concurrent reduction of Cu^{2+} and H^+ ions at the cathode electrode in the HEA process produces a stream of fluid toward the electrodes due to the hydrogen bubble release [21], [59]. The fluid motion (convection) assists the motion of copper ions beyond the limited diffusion rate [22]. Also, the local electric field between the two cathodes supports the migration mechanism for faster lateral deposition. While both convection and migration have direct influences on the deposition rate, the main reason for the fast rate of deposition is the porous structure of the copper (i.e., low density).

Hydrogen evolved at the cathode causing the structure of the electroplated layer to be more porous due to the agglomeration of bubbles from different sizes because of coalescence of bubbles [29], [42],[54]. As SEM images suggested previously, the variation in the growth rate for different concentration of acid and CuSO_4 is mainly due to the difference in the nanostructure of the grown

copper. Increasing the acid concentration from 0.125 to 1.5 M results in higher concentration of H^+ ions in the electrolyte that affected the size and distribution of hydrogen bubbles that were formed on the cathode electrode, leading to the formation of open porous [60],[41],[58]. Larger hydrogen bubbles produced larger void area and reduced the density of the deposited copper. However, beyond 1.5 M the deposition rate was significantly lower. The exact reason for the lower rate is not known yet and needs further study. However, the loose electric contact between nanostructures when the bubbles are relatively large, and a lower kinetic rate of copper reduction are likely the reasons for lower rates of copper deposition at high concentrations of acid.

Although the results clearly show the effect of the electrolyte concentration on the copper nanostructure and the growth rate, to reproduce the results for obtaining the same growth rates, other factors such as the geometry of the electrochemical cell and arrangement of the electrodes should be considered. Changing the cell geometry or the electrode arrangement can directly affect the hydrogen bubble formation and release on the cathode which would change the conditions of the HEA process. Nevertheless, the presented results are promising for developing a printing method through which copper can be directly printed on fabric and plastic substrates for applications in wearable and flexible electronics.

4.4 Conclusion

The lateral copper growth assisted by hydrogen evolution electroplating was studied using the HEA method to promote a faster deposition of copper on PCB samples proving to be efficient for lateral growth of copper on the substrate of the electrodes. The study results show that the concentrations of acid and $CuSO_4$ have a direct effect on the copper growth, due to the change in the density of the electrodeposited copper. The fastest growth rate of $15.6 \mu m s^{-1}$ was obtained for an electrolyte containing 0.15 M $CuSO_4$ and 1.5 M of H_2SO_4 . The SEM images showed a

higher density of the copper nanostructures at a low acid concentration at which a slow growth rate was observed. The agglomeration of hydrogen bubbles over the surface of the working electrode, while copper was being plated, was a factor that affected the growth rate and nanostructures of copper. Also, the HEA method was successfully employed for soldering an electronic component to a copper track, proving the possibility of fabricating electronic circuits with this method on various substrates. Further studies are encouraged to identify the critical parameters in controlling the HEA process to develop a reliable copper printing method for obtaining reproducible growth rates.

Chapter 5: Copper Electrodeposition by Hydrogen Evolution Assisted Electroplating (HEA) for Wearable Electronics ³

5.1 Introduction

Along with advantages in the development of wearable and flexible electronics, there is an increasing demand for lightweight, flexible, and wearable human and environmental monitoring systems with countless applications [13]. Among different technologies and approaches, patterning a conductive template (i.e., circuit layout) on fabrics by copper electrodeposition wearable technology market, which has propelled itself as one of the most discussed topics in the field during past few years can lead to the development of different wearable and flexible electronics. Leading to a variety of technologies such as smart watches, health trackers, smart clothes, providing advances not only at the scientific level but developing a positive impact in areas of medicine, military advances, among others. Since the market is predicted to develop from its present-day value of USD 40 billion to a full-size price of USD 160 billion through 2026, the ability for novel concepts of wearable technologies is surely visible [11]. With technology development, integrated circuits (ICs) have become more compact, lightweight, and low-power, well suitable for integration of ICs into fabrics for development of e-textile and wearable electronics. Currently, there is a huge interest in developing wearable medical devices for constant monitoring health status of patients, smart soldier vests for carrying more gadgets, and smart textiles for monitoring recreational activities [61], [62].

³ This chapter was published before in IEEE-2020 Pan Pacific proceedings (Sabrina M Rosa-Ortiz, Arash Takshi, "Copper Electrodeposition by Hydrogen Evolution Assisted Electroplating (HEA) for Wearable Electronics", 2020 Pan Pacific Microelectronics Symposium (Pan Pacific) (2020), 1-5). Permission is included in Appendix I.

Although, the IC technology is well developed to address the needs in medical, military, and recreational applications, the lack of any practical solution to integrate devices to fabrics has limited the approach to the fabrication of printed circuit boards separately and using glue or a Velcro-type mechanism for the attachment, not suitable for truly e-textile applications.

Developing e-textiles demands a fabrication method to integrate electronic components and circuits into fabric structures with the interconnect conductivity as high as that in copper ($\sim 6 \times 10^7$ S/m) and a printing method with the feature size less than 1 mm to be compatible with the packaging of surface mount devices (SMDs) [14]. In addition, the adaptation of the current available devices and attachment-based wearables into integrated technology may involve a significant size reduction while retaining their functional capabilities [13]. The recently devised HEA method can electroplate the surface of a conductive pattern with a growth rate of at least four orders of magnitude faster than the conventional galvanostatic electroplating speed and produces nanostructures for embedding the printed structure to the fabric fibers [63]. More importantly, it is feasible to solder electronic components to the printed circuit board (PCB) at a low temperature by the HEA method [5], [16]. Surface modification of textiles with desired functionalities can be engineered by a considerable number of techniques ranging from traditional treatments to multifunctional approaches. Textiles, in fact, offer a challenging platform for functional modifications to meet additional strategic requirements for a large variety of applications [17].

Wearable electronics consists of fabrics that feature electronics and interconnections woven into them, supplying physical flexibility and normal size that cannot be performed with different existing electronic production strategies. The usage of e-textiles has shown a rapid adjustment and adaptation within the computational and sensing requirements of any particular utility.

As shown in table 1, the fabrication of wearable electronics can lead us to obtain a numerous amount of characteristics and functions based on the approach used for its development. The main goal of using wearable electronic systems as our everyday outfits must meet special requirements concerning wearability. Wearable systems will be characterized by their ability to automatically recognize the activity and the behavioral status of their own user as well as of the situation around her/him, and to use this information to adjust the systems' configuration and functionality. The convergence of textiles and electronics (e-textiles) can be relevant for the development of smart materials that can accomplish a wide spectrum of functions, found in rigid and non-flexible electronic products nowadays [64].

Table 3. Different methods of fabricating e-textiles

Method	conductivity	flexibility	cost	resolution	distributed*	soldering
Sewn (metallic wires)	✓	✗	✓	✓	✓	✗
woven/knitted (metallic wires)	✓	✗	✗	✓	✓	✗
woven/knitted (conductive yarns)	✗	✓	✗	✓	✓	✗
Silk screen	✗	✓	✓	✗	✗	✗
Inkjet	✗	✓	✓	✗	✗	✗
Attached PCBs	✓	✗	✓	✓	✗	✗
Proposed method	✓	✓	✓	✓	✓	✓

5.2 Experimental

5.2.1 Materials

5.2.1.1 Textiles

The 1000 Denier Coated Cordura Nylon, Laminated Polyester Ripstop and 100% Virgin Vinyl textiles were purchased from Rockywoods Fabrics. Each type of fabric was used placing

conductive track of MWCNTS over them to conduct the experiments. The size of each sample of fabric used was of approximately 3.2 cm x 3.2 cm.

5.2.1.2 Interconnection Track

Multiwalled carbon nanotubes and Sodium dodecylbenzenesulfonate (SDBS) from Sigma Aldrich were used to develop an ink to be used as the interconnection track over the fabrics. The MWCNT ink was fabricated as mentioned by Aljafari et al. by adding 300mg of MWCNTs and 150mg of SDBS into 30 mL of DI water [65]. A desktop ultrasonic processor was used to make a homogenous mixture of the MWCNTs and SDBS. The solution was sonicated for 30 minutes at 30 W and 40 J. To make the interconnection track over each textile type a 5 mL disposable syringe was used. The fabrics were placed in the furnace for 5 minutes at 120 degrees Celsius, then removed and repeated for four times.

5.2.1.3 Electrolyte

To study the Hydrogen Evolution Assisted electroplating over the MWCNTs ink track, an aqueous solution containing 0.47 M CuSO_4 and 1.5 M H_2SO_4 (both from Sigma-Aldrich) was prepared by mixing them with 10mL of DI water for 5 minutes until completely dissolved.

5.2.2 Sample Preparation

To study the deposition of copper by the interaction of the hydrogen bubbles released while the deposition is taking place, a MWCNT ink track of 0.1 mm was made over each textile being studied. One of the main challenges of creating conductive patterns on fabrics [66] and soldering electronic elements is the damage it causes to use soldering paste or soldering wire with a heating tool (i.e., soldering iron or heat gun) which melts the solder (typical temperature of 300 °C) which then spreads into the fabric. The heat can damage the fabric, and the diffused solder changes

significantly the stiffness of the fabrics at the soldering joints, and most of all, make a poor electric connection at the joint. For that reason, almost all the reported wearable electronics have used a form of a conductive paste (mainly silver pastes) for soldering. The low durability of pastes on flexible substrates can fail the entire integrated electronic system with only one poor soldering joint. To prevent the damage of the fabrics and to allow the variation of voltage interacting with the sample, two cables were sewed to the fabric to make a proper connection and to work as the working electrode using sewing thread and metallic thread as shown in figure 13.



Figure 13. A schematic of a piece of fabric with MWCNT track and connection cables properly sewed to provide continuous connection between the fabric and the instrument.

To allow the transport of Cu^{2+} ions in the aqueous solution a copper coil of 0.25 cm diameter was used as the counter electrode. Using an O-ring of 0.8 cm diameter, a small electrochemical bath was formed around the cathode. An aqueous based $\text{CuSO}_4 + \text{H}_2\text{SO}_4$ electrolyte and a copper wire anode (inserted into the bath) were used for the deposition. A microscope camera was set on top of the cell to record the process.

5.3 Results and Discussion

Applying a variation in voltage of -0.5 V to -2.0 V hydrogen bubbles appeared near the cathode, while a porous structure of copper started to grow as shown in figure 14. Variation of the voltage has been tested to understand the effect of the voltage and the conductivity of the copper

deposition to find the best combination for the fastest electroplating growth with the lowest resistance of the final conductive structure on the surface.

A constant and continuous growth was observed for both types of fabrics showing a proper adhesion of the copper deposits for 1000 Denier Coated Cordura Nylon in Figure 14a and Laminated Polyester Ripstop in Figure 14b as well as the presence of the hydrogen evolution assisted electroplating which helped in the fastest deposition of copper allowing a wider agglomeration over the MWCNTs. As for the 1000 Denier Coated Cordura Nylon the agglomeration of copper deposits was significant, for the Laminated Polyester Ripstop the copper growth was more continue and less influenced by the hydrogen evolution which can be caused by the type of arrangement of the fabric's fibers. As shown in figure 15 the structure of the Laminated Polyester Ripstop fabric is very continuous.

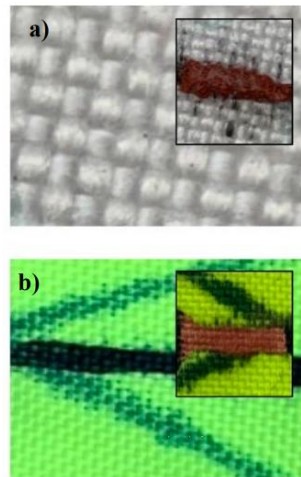


Figure 14. a) 1000 Denier Coated Cordura Nylon and b) Laminated Polyester Ripstop fabrics before and after copper electrodeposition takes place.

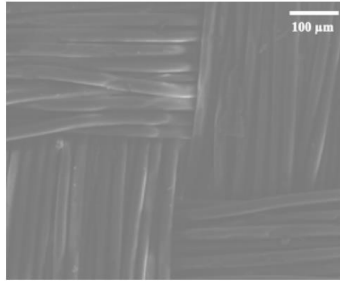


Figure 15. Structure of the Laminated Polyester Ripstop fabric at 100 μm

The SEM image of the HEA grown copper (Figure 16a and 16b) shows that the structure is highly porous and present nanoscale features for the 1000 Denier Coated Cordura Nylon fabric while for the Laminated Polyester Ripstop the copper deposition is more segregated creating a smoother structure. It is found that the shape of the nanostructures is a function of the concentration of the electrolyte and the applied voltage.

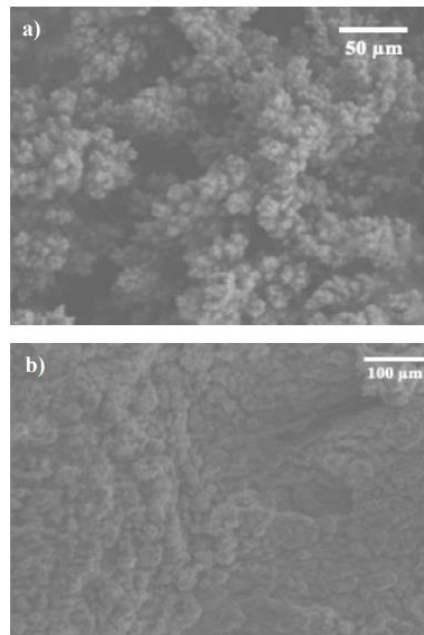


Figure 16. a) 1000 Denier Coated Cordura Nylon at 50 μm showing copper with a cauliflower structure after deposition and b) Laminated Polyester Ripstop fabrics after copper electrodeposition showing a more uniform structure with some copper agglomeration.

The proposed fabrication method aims to address some challenges in the current technologies by offering a relatively low-cost patterning of continuous high-resolution (suitable for SMDs) conductive interconnects at a high conductivity and a reliable method of soldering SMDs directly to the fabricated circuit layout. The HEA electroplating has an incredible speed of growing metals compared to the conventional electroplating generating structures of copper on the deposited area that can entangle the conductive pattern to the fabric for improving the adhesion of components and the integration of circuits.

Localized HEA electroplating to develop a new approach for e-textile fabrication by integration of electronic circuits into fabrics to address the market need for smart textiles. In a simple approach, also known as embroidered circuits, conductive yarns/threads are sewn for interconnecting the electronic elements [67]. In a more advanced level, conductive threads can be woven or knitted during the production of the fabric to make the conductive circuit layout [66][68]. Woven or knitted e-textiles are more expensive and limited in the applications than additive methods for integration of electronics on already fabricated textiles. In all these approaches, the trade-off is between the flexibility of the final circuit and the conductivity of interconnects. Using metallic wires as the threads/yarns provide an excellent conductivity, but stiffness difference between wires and regular threads limits the flexibility of the final product. Using regular yarn materials, coated with conductive inks, maintains the flexibility of the fabric, but their low conductivity is not suitable for distributed electronics on fabrics; thus, the need for this work.

Many efforts have been put into fabricating wearable electronics by applying the circuit layout on fabrics with a printing method using conductive inks. Iron-on, silk screen, and inkjet printing methods have been demonstrated before [64], [69], [70]. In general, Iron-on and silk-screen patterns on fabrics have low printing resolutions not being suitable for patterning

interconnects between terminals of SMDs with less than 1 mm spacing. Although the current inkjet printing technology offers high resolutions suitable for simple circuits, the conductivity of the printed patterns at high printing resolutions is too low for true e-textiles which may include embedded sensors, microprocessors, and wireless chips distributed all over the surface of a piece of clothing [64] [71]. This is mainly due to the principle of printing patterns via printing droplets of ink containing metallic particles or conducting polymers.

At the microscopic level, after drying the ink, only a high level of overlapping (above the percolation level of the conductive particles) can generate an electrically conductive pattern at the macroscopic level [69]. In case of metallic nanoparticles, after printing, particles must be sintered [72]. Considering the dispersion of ink on the fabric fibers and a high porosity of fabrics, the yield of printing electrically continuous interconnects with high resolution is very low. For the same reason, even, at lower resolutions, the resistance of the interconnects is often too high for advanced electronics. Localized HEA electroplating to develop a new approach for e-textile fabrication by integration of electronic circuits into fabrics has the potential to revolutionize the wearable electronics industry for production of miniaturized integrated electronics for medical, military, and recreational applications.

5.4 Conclusion

Copper electrodeposition assisted by the hydrogen evolution technique at voltage variation of -0.5 V to -2.0 V had shown a constant and uniform copper growth suitable for printing a circuit layout, soldering components, and creating integrated circuits into fabrics. The hydrogen evolution effect was observed during the electrodeposition resulting in a dramatic increase of copper deposition while the electroplating was taking place. Due to the agglomerations of hydrogen bubbles a more porous copper structure was observed while using the 1000 Denier Coated Cordura

Nylon fabric instead of a more compact structure as observed while using Laminated Polyester Ripstop fabric. Although the porous copper structure was not as uniform as we were expecting significant advantage of the HEA electroplating method can be gain from this structure. As it was shown copper electrodeposition over fabrics is a viable method which does not require any soldering machine to achieve a proper metal deposition facilitating the commercialization and development of several applications.

Chapter 6: Advances in Lateral Copper Electroplated Metallic Tracks—Production and Applications by Using Hydrogen Evolution Assisted Electroplating⁴

6.1 Introduction

Copper has been used as one of many materials for plating over non-metallic and metallic surfaces. It has allowed a broad range of applications in many industries such as in the manufacturing of electronic components, automobile, biomedical and aerospace. Having a participation and great contribution as well as in the incorporation of electronic components and the development of integrated circuits in cellphones, computer, wearable electronics, and other electronic devices thanks to its ability to combine its properties with the surface properties of the substrates being used. To assure that the properties of copper are being used to the maximum, the electrochemical technique known as electroplating has been incorporated allowing the enhancement of electronic parts and device applications to the desire size and thickness by coating a surface with a layer of metal. The usage of this technique for the development of devices and electronics is seen as responsible for the increasing number and widening types of applications allowing an increment of economy and convenience by the prevention of corrosion, and by permitting a significant increment of the electrical conductivity.

Over the years, flexible devices and wearable systems have gained significant attention in the scientific and commercial field. Yet, a challenge is in the development and integration of electrodes at any desired shape and size with enough flexibility and electrical conductivity suitable

⁴ This chapter was published before in MRS Advances, 2021 – Springer (Sabrina M Rosa-Ortiz, Arash Takshi, Sylvia Thomas “Advances in lateral copper electroplated metallic tracks—production and applications by using hydrogen evolution-assisted electroplating”, 2021 MRS Spring Meeting. Permission is included in Appendix I.

for flexible and wearable electronics [12]. With the developing technologies at a worldwide level electronic textile are emerging cutting across traditional industrial procedures. The development of flexible materials is essential for wearable electronics because of their unique chemical, electrical, and mechanical properties. Replacing relatively poor mechanical flexibility and stretchability such that they can be conformally attached onto the human body for clothing, communication, healthcare monitoring, military, sensors, among others playing a key role among various technologies. Based on the rapidly changing global demands, the development of responsive functionality on textiles has led to the emergence of the revolution we are seeing in the field of wearable electronics [73]–[75]. The merging of textiles technologies has the potential to combine the positive attributes of each technology playing an important role in determining the characteristics, cost, and stability of the flexible and wearable electronics [76] while aiming for highly flexible, stretchable, and adaptable to comport to frequent deformations during usage in daily life [77].

Carbon materials have recently brought attention due to their natural abundance, structural properties, and mechanical bendability allowing to surpass current factors in the limitation of the growth of flexible and malleable materials [78]. Its significant properties have allowed us to use the multiwall carbon nanotubes as electrode over a variety of fabrics employing the novel technique called HEA electroplating, to enhance the lateral deposition of copper and its properties leading to the development of useful wearable electronics with the goal of overcome the existing challenges and create future opportunities[79][80]. The usage of copper as part of the electrodeposition technique to enhance properties and promote better production and development of applications can be obtain by the application of a potential using a VersaSTAT 4.0 potentiostat. Promoting not only the deposition of this metal but also improving it by the application of a

variation in voltage. This variation allows a better deposition over the surface of the substrate and more time for the surface to receive the copper grains from the interaction of hydrogen bubbles due to the electrolysis in the electrolyte solution. This technique provides an increment in the growth rate of copper in comparison with the conventional galvanostatic technique, also promoting a better incorporation of the morphology of copper over the substrate after its deposition [5].

6.2 Experimental

Samples were made by using 100% Virgin Vinyl, 1000 Denier Coated Cordura Nylon and Laminated Polyester Ripstop purchased from Rockywoods Fabrics, with a size of 3.2 cm x 3.2 cm. To create an electrode over the fabric a conductive track, multiwall carbon nanotubes and Sodium dodecyl-benzenesulfonate (SDBS) were used to develop the ink that will work later as the electrode. The MWCNT ink was fabricated as mention by Aljafari et al. [65] and Rosa-Ortiz et. al. [79] by adding 300mg of MWCNTs and 150mg of SDBS into 30 mL of DI water and sonicated to make a homogenous mixture of the MWCNTs and SDBS. To pattern the conductive track over the fabrics a 5 mL disposable syringe was used and tape to prevent the ink from spreading over the fabric. Each fabric was places in the oven for 5 minutes at 120 degrees Celsius, then removed to apply the ink again and place in the oven for a total of four times. To conduct the experiment an electrolyte solution containing 0.47 M CuSO_4 and 1.5 M H_2SO_4 (both from Sigma-Aldrich) [5] was used to complete the electrochemical cell. To obtain the lateral copper electrodeposition by hydrogen evolution a variation in voltage between -0.8V to -1.3V was applied using a VersaSTAT 4.0 potentiostat to conduct the cyclic voltammetry technique.

6.3 Results and Discussion

The usage of fabrics like 100% Virgin Vinyl as shown in Figure 17 as a substrate to give place to the process of copper electrodeposition assisted by hydrogen evolution has allowed us to incorporate carbon nanotubes as electrodes as shown in Figure 17b providing mechanical and electrical support, with a unique one-dimensional structure [81]. To obtain the lateral copper electrodeposition by hydrogen evolution a variation in voltage between -0.8V to -1.3V was applied using a VersaSTAT 4.0 potentiostat to conduct the cyclic voltammetry technique. To further study the impact of copper being deposited by the electroplating technique the electrical conductivity of the carbon pattern was measured before the electroplating and after copper metallization as shown in table 4 where the 100% Virgin Vinyl showed the higher conductivity (σ) after the copper electrodeposition while the 1000 Denier Coated Cordura Nylon showed the lowest conductivity after deposition but with an increment of almost 10 times the conductivity in its fabric in comparison with its measurement before deposition. In the three fabrics there was a significant increment before and after the copper electrodeposition was made over each fabric, meaning that the process allows to enhance the conductivity allowing the proper usage of fabrics as substrate for significant applications. The growth of copper electrodeposition was rapidly spotted and the complete coverage of the MWCNT electrode was observed as shown in Figure 16b having a growth rate of 99.57 $\mu\text{m/s}$.

Table 4. Conductivity measurements for the fabrics before and after the copper electrodeposition

Fabric	Conductivity(σ) before deposition	Conductivity(σ) after deposition
100% Virgin Vinyl	0.05 S/m	0.17 S/m
Laminated Polyester Ripstop	0.014 S/m	0.05 S/m
1000 Denier Coated Cordura Nylon	0.001 S/m	0.012 S/m

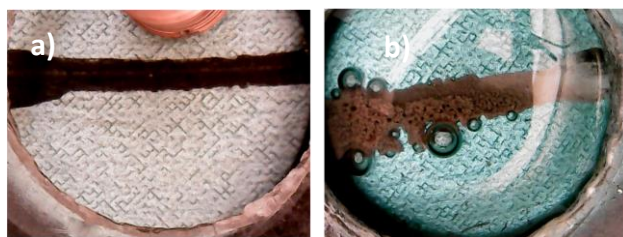


Figure 17. Optical microscope image of the 100% Virgin Vinyl fabric with the MWCNTs conductive template a) before and b) during the electroplating process.

The laminated polyester ripstop fabric as shown in Figure 18a was also used since it is a versatile material that provide thermal properties and is known for its durability. To complete the electrochemical cell each sample had a copper wire with a diameter of 0.23 cm used as the counter electrode to provide the copper for the electrodeposition over the MWCNT electrode as seen in Figure 18b also known as working electrode.

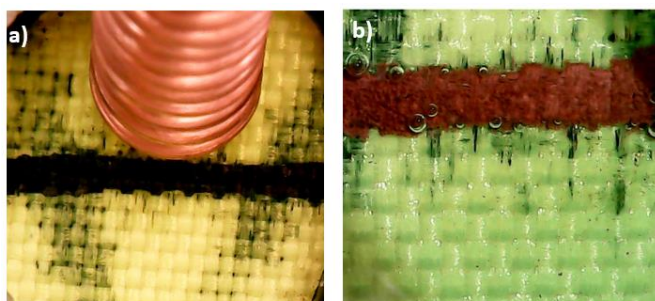


Figure 18. Optical microscope image of the Laminated Polyester Ripstop fabric with the MWCNTs conductive template a) before and b) during the electroplating process.

The 1000 Denier Coated Cordura Nylon fabric is well known for being a strong, resistant, and durable material sometimes created from a synthetic blend or a synthetic and cotton combination, mostly used for military gear and clothing. The sample used for the electrochemical procedure as shown in Figure 19a shows a surface which is not completely smooth which we thought would be an impediment at the time of performing the lateral copper electrodeposition over the MWCNTs trace (as shown in Figure 19b) which turned out to be false since in this fabric it is possible to obtain the greatest deposition of copper in the shortest possible time having the

best growth rate among all three fabrics. The bubbles over the copper that has been deposited represent the hydrogen bubbles that were released after electrolysis was achieved, permitting a faster transport and mobility of the copper ions toward the substrate to create a metallic layer of copper. These bubbles collide with each other and join by a process called coalescence, giving way to a variety of structures in copper.

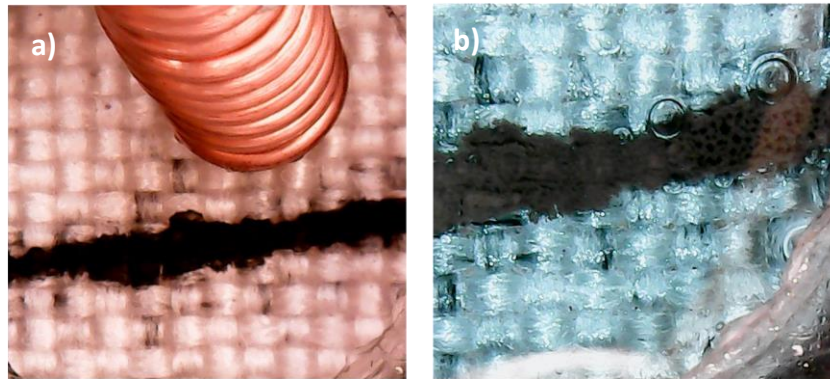


Figure 19. Optical microscope image of the 1000 Denier Coated Cordura Nylon fabric with the MWCNTs conductive template a) before and b) during the electroplating process.

It has been shown that by applying a varying voltage we can allow greater deposition of copper on the substrates since this allows a break in the agglomeration of hydrogen bubbles on the surface giving space for more copper ions to move the substrate and reduce as copper metal. This allows us to obtain a variety of copper morphologies being directly affected by voltage, acid concentration in the electrolyte and by the direct interaction of hydrogen bubbles. Being able to vary each of the previously mentioned elements allows us to adjust to a certain extent the desired morphology of copper to implement applications. After completion of the electrodeposition over the 1000 Denier Coated Cordura Nylon fabric, which reported the fastest growth rate of copper, we were able to observe with naked eyes honeycomb like structure over the substrate created by the agglomeration of hydrogen bubbles throughout the process.

At 100 μm as shown in Figure 20a we observed a structure with more trend towards dendrites with a mixture of cauliflower like structure but when magnifying up to 50 μm we were able to see that the morphology of copper leading the formation of the whole honeycomb like structure of the lateral deposits were supported by cauliflower like structure as shown in Figure 20b which is a result of the voltage being applied towards the sample.

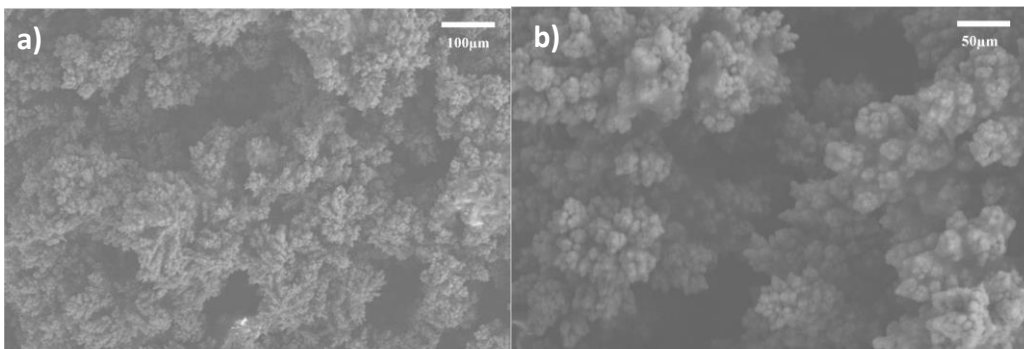


Figure 20. a) Observation of dendrite and cauliflower formations over a 1000 Denier Coated Cordura Nylon fabric at 100 μm using an SEM Hitachi S-800, b) Cauliflower structure of 1000 Denier Coated Cordura Nylon fabric at 50 μm

The incorporation of hydrogen evolution to obtain the lateral copper electrodeposition was done by the application of a variation in potential ranging from -0.8V to -1.3V with a scan rate of 50mV/s using a VersaSTAT 4.0 potentiostat. As shown in Figure 21, 1000 Denier Coated Cordura Nylon has only three cycles in comparison with the Laminated Polyester Ripstop and 100% Virgin Vinyl, this is due to the fast growth of copper over the fabric which only needed 10 cycles to complete the lateral copper electrodeposition over the MWCNTs track and showed an increase in current greater than the one for other fabrics. However, for the 100% Virgin Vinyl the copper growth took longer showing an increment in current but even so, this increase was less than the one observed for Laminated Polyester Ripstop and 1000 Denier Coated Cordura Nylon which were around -8.5mA and -9.5 mA.

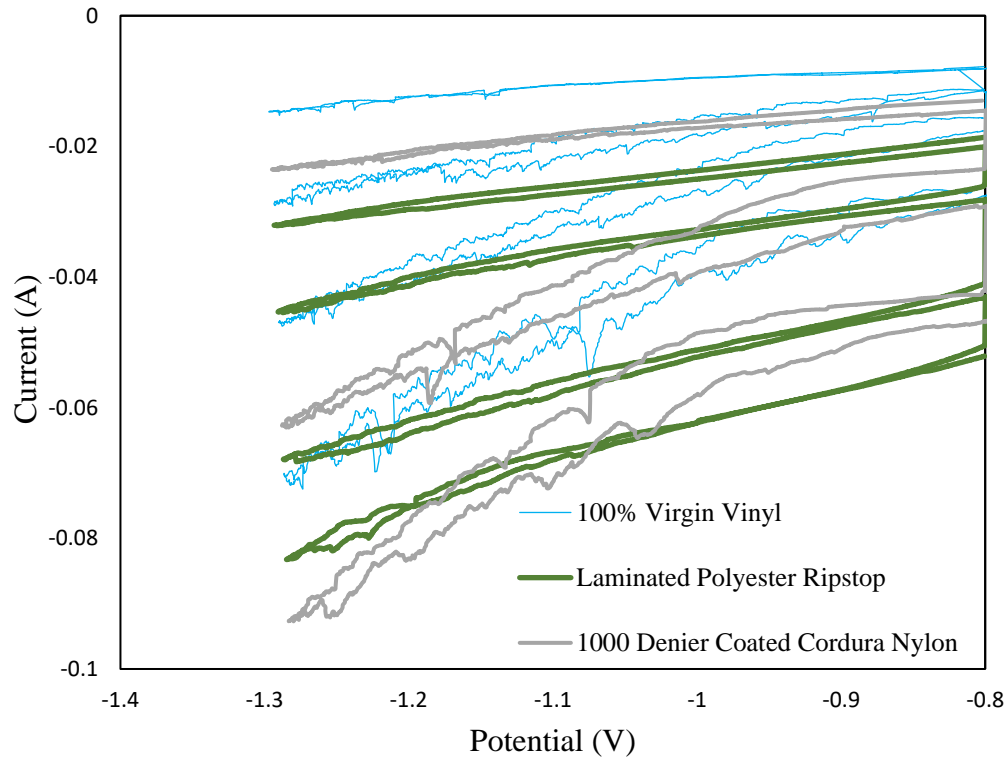


Figure 21. Cyclic voltammetry result for 1000 Denier Coated Cordura Nylon, Laminated Polyester Ripstop and 100% Virgin Vinyl

6.4 Conclusion

The impact of hydrogen evolution assisted electroplating over the lateral growth of copper was studied using the cyclic voltammetry technique to assure a better quality of deposition by a variation in the potential range being applied. The usage of this technique allowed a better lateral deposition and an enhancement in the growth rate of copper since it allowed the hydrogen bubbles interacting with the substrate to be detached granting more transport of the copper grain towards the working electrode.

Chapter 7: Hydrogen Evolution Assisted Cyclic Electroplating for Lateral Copper Growth in Wearable Electronics⁵

7.1 Introduction

In 1840 the electrodeposition process was introduced as a manufacturing technique where an anode was used to ensure passage of current through the electroplating cell for the deposition [82]. With the development in electronic devices, Cu electrodeposition has been used widely for fabricating printed circuit boards (PCBs) and many other electronic components [83], [84]. Electrodeposition of metals is the most cost-effective way to achieve deposition commonly used in the electronics manufacturing industry mainly to achieve high density interconnects in PCBs [1], [2]. Metallization of substrates by copper electrodeposition enhances the electric conductivity of their surfaces potentially leading to an improvement of their electron transfer and a direct impact on the growth rate of the metal being plated [6].

In the conventional copper electroplating, using an electrochemical cell, a few hundred millivolts are applied between a copper counter electrode (anode) and the working electrode (cathode) [85]. The passage of current through the cell forces the movement of ions [82]. In general, the motion of ions in the electrolyte is governed by diffusion, migration, and convection [22]. Once the ions are near the working electrodes area, the migration and convection are negligible, and the growth rate of the copper is dominated by the diffusion of ions from the bulk

⁵ This chapter was published before in the Journal of Electroanalytical Chemistry (Sabrina Rosa-Ortiz; Kat-Kim Phan; Nida Khattak; Sylvia W Thomas; Arash Takshi), “Hydrogen Evolution Assisted Cyclic Electroplating for Lateral Copper Growth in Wearable Electronics”, Journal of Applied Electrochemistry (2021). Permission is included in Appendix I.

solution towards the surface of the working electrode. The growth rate and quality of the deposition are both affected by the speed at which copper ions reach the cathode [1]. The restriction imposed by the ions mass transfer in the cell usually results in a slow copper growth in a galvanostatic or potentiostatic deposition modes (i.e., constant current or voltage) [5]. To enhance the deposition rate, a large overpotential can be applied across the cell. However, as we have shown in our previous work, application of a constant DC voltage higher than 1.23 V leads to the release of hydrogen bubbles at the working electrodes producing a porous structure of copper [5], [16]. This method of electroplating is known as hydrogen evolution assisted (HEA) mode. The consequence of concurrent reduction of Cu^{2+} and H^+ at the cathode is an incredible speed of growth due to convection of copper ions and more importantly formation of a porous copper layer instead of a compact deposition [20], [21]. The main problem with applying a constant voltage is that there is no control of the hydrogen bubbles being released and interacting with the surface of the working electrode [5]. The constant interaction of the hydrogen bubbles restricts the complete deposition of copper which also creates a limitation at the electrode-electrolyte interface for an effective charge transfer to the cations, ultimately stopping the deposition.

As a solution to this restriction and to produce more uniform and predictable nanostructure, instead of a constant voltage, in this work, we have superimposed an alternating voltage to the DC voltage. By alternating the voltage above and below 1.23 V, in a portion of each cycle when the hydrogen evolution occurred, a high growth rate was achieved. The rest of each cycle gave time for the generated bubbles to leave the surface. We have studied the effect of the frequency of the AC voltage and the magnitude of the DC and AC voltages on the lateral growth speed and the quality of the deposited layer.

To superimpose the alternating voltage to the DC, the cyclic voltammetry (CV) mode was used in which a triangle wavelshape AC with a constant voltage scan rate was applied [6].

7.2 Experimental

7.2.1 Electrochemical Cell and Sample Preparation

As shown in Figure 22a, the working electrodes with a gap of 1 mm were made by etching FR-4 PCB boards in a ferric chloride etching solution. The pattern was applied using a permanent marker. After etching, the electrodes were immersed in acetone for 1 minute to remove the permanent marker ink. Then, it was washed with water to remove any residue left. The samples were properly dried and polished with sandpaper to remove any marks over the surface. Two pieces of wires were soldered to the copper pads for easy connection to the instrument. A piece of copper wire with diameter measures of 0.23 cm was used throughout the work as the counter electrode 2 mL of an electrolyte made of CuSO_4 (0.47 M) and H_2SO_4 (1.5 M) in deionized water was used with the working and the counter electrodes to assemble the electrochemical cell. To properly hold the electrolyte, an O-ring of 2.54 cm diameter was placed between the two pieces of plexiglass that completed the cell (Figure 22a).

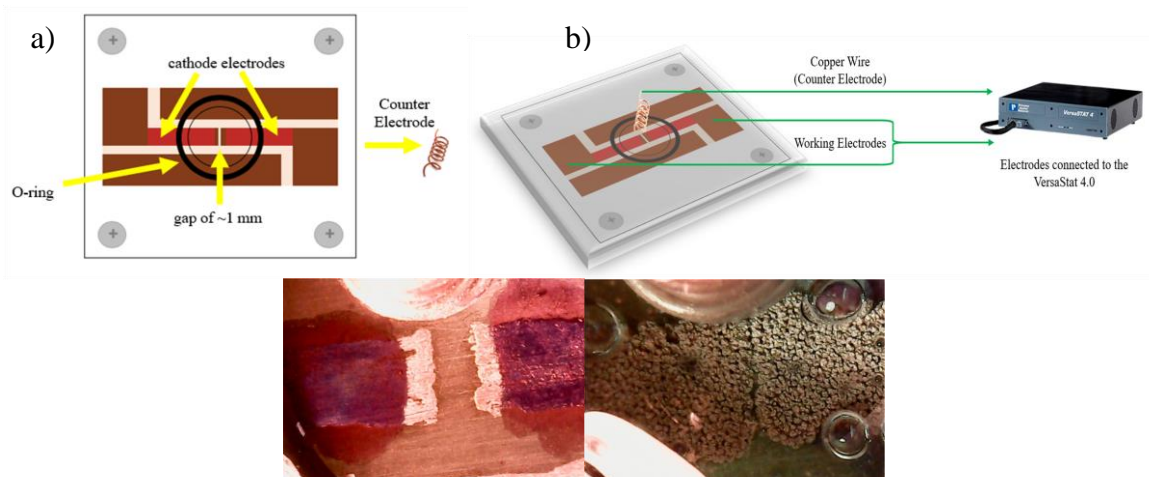


Figure 22. a) Schematic of the working and counter electrodes on a PCB, b) schematic of the connection of the electrodes with the VersaStat 4.0 instrument, c) lateral growth before and after the copper electrodeposition

7.2.2 Electrochemical and Electrical Measurements

The copper growth was conducted using the CV method at different voltage ranges and scan rates. Specifically, four different ranges were studied: a) from -0.8 V to -1.3 V ($V_{DC}=-1.05$ V and amplitude AC of $V_{AC}=0.25$ V), b) from -0.8 V to -1.5 V ($V_{DC}=-1.15$ V and $V_{AC}=0.35$ V), c) from -1.0 V to -1.3 V ($V_{DC}=-1.15$ V and $V_{AC}=0.15$ V), and d) from -1.0 V to -1.5 V ($V_{DC}=-1.25$ V and $V_{AC}=0.25$ V). For each case, samples were tested at scan rates of 5 mV/s, 10 mV/s, 20 mV/s, 50 mV/s, 100 mV/s, 300 mV/s, and 500 mV/s using VersaStat 4.0 potentiostat in a two-electrode configuration. As shown in Figure 22b, both working electrodes were connected. The lateral growth was monitored by video recording the electroplating process using a digital microscope (Figure 22c). The lateral growth rate was estimated through the recorded videos by measuring the time that it took for the copper to grow across the 1 mm gap.

7.2.3 Morphology analysis

The surface morphology was observed by a Quanta 200 3D Dual Beam scanning electron microscope (SEM).

7.3 Results and Discussion

Figure 22 shows the second loop of the CV results for seven samples that were tested for a voltage range between -0.8 V and -1.3 V at different scan rates. The number of cycles were different in different experiments based on the speed of growing copper across the gap. At very low scan rates (i.e., 5 mV/s and 10 mV/s), when the frequency of the AC was very low, the situation was similar to the DC growth condition reported in our previous work[5]. In the DC case, the generated hydrogen bubbles almost blocked the surface of the cathodes and limited the access of the Cu^{2+} to the electrodes for further electrodeposition. Because of that the current level was almost constant at -60 mA for 5 mV/s and -80 mA for 10 mV/s. It was observed that when the frequency

of the AC was increased (faster scan rates), the CV loops presented two distinct sections. The first section, closer to -0.8 V, was without hydrogen evolution that presented smooth curves with a shallow slope of the current. However, the second part of each curve closer to -1.3 V occurred when the hydrogen bubbles were released as the copper was growing. The effect of hydrogen evolution was to enhance the copper growth which resulted in a sharper slope in the current. Also, the disturbance due to the hydrogen bubbling generated a relatively large ripple in the current as the voltage was scanned. Exceptions are at very fast scan rates of 300 mV/s and 500 mV/s in which scanning the voltage back and forth between -0.8 V and -1.3 V took only a few seconds with almost no ripple in the current. Similar features as presented in Figure 23 were observed in the CV results when samples were tested under different DC and AC voltages.

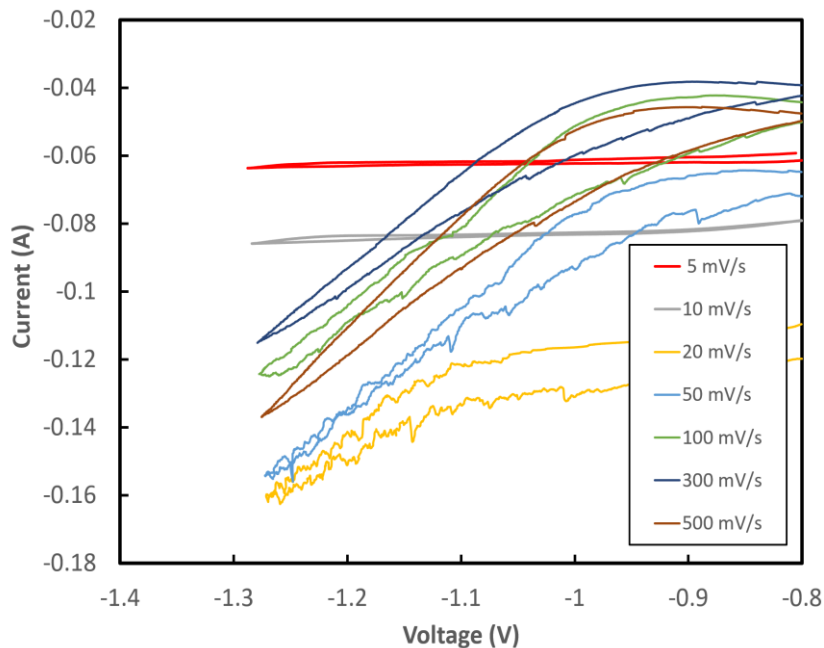


Figure 23. CV results for the samples grown between -0.8 V and -1.3 V at different scan rates. Only the second cycle are presented.

To find correlations between the voltages (V_{DC} and V_{AC}) and the lateral growth rates, the growth rate for each sample was estimated from the time that it took for the copper to bridge the gap and was plotted versus the frequency of the AC voltage. The frequency was calculated from the period of each cycle in the CV experiments. The estimated growth rate from all the samples in cases 'a'-'d' at different frequencies are shown in Figure 24.

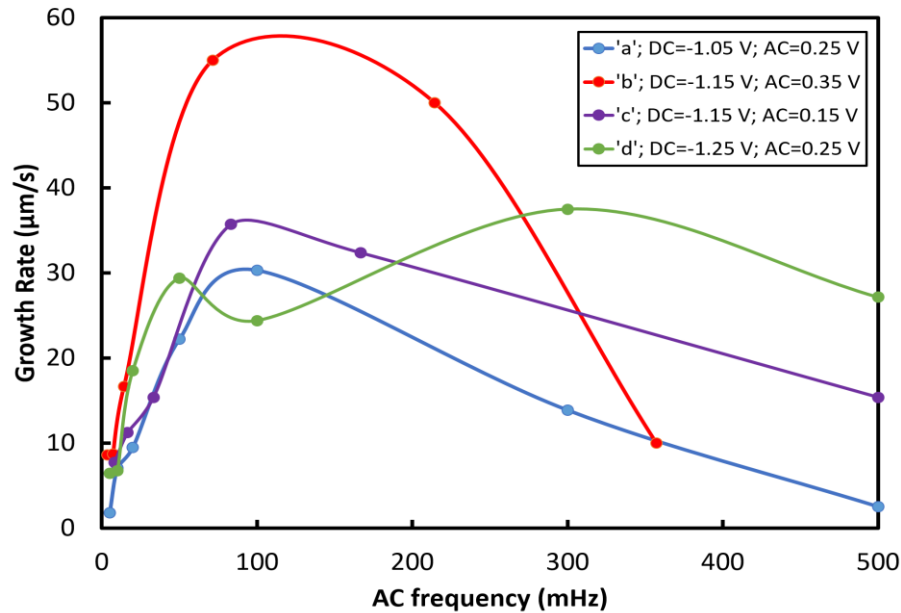


Figure 24. Copper lateral growth rate vs. the frequency of the AC for different V_{DC} and V_{AC} amplitudes as defined in cases a-d.

The results clearly show that the growth rate is very slow at low frequencies (i.e., slow scan rates). By increasing the frequencies, almost the fastest growth rate is achieved around 100 mHz, except for case 'd', in which the fastest rate occurred at 300 mHz. An interesting aspect of the results is the decrease in the growth rate with an increase in the frequencies. Among all different growth conditions, the fastest rate of $55 \mu\text{m/s}$ was achieved in case 'b' (voltage range of -0.8 V and -1.5 V) at 71.5 mHz frequency.

To understand the difference in the growth processes in different cases, the voltage variations vs. time are plotted for all four cases in Figure 5. Since water electrolysis at 1.23 V, the -1.23 V level is shown in the plots as a reference to the boundary for starting the hydrogen evolution near the cathodes. It should be noted that, in practice, the transition between HEA and non-HEA mode is not a binary transition, but a strong electrolysis is expected at -1.23 V and lower. Hence, the part of the voltage in each cycle with a value less than -1.23 V is marked with a shaded triangle, indicating the expected HEA electroplating.

Case 'a' shows that, regardless of the frequency, HEA covers a small fraction of each cycle. Also, the large voltage difference between $V_{DC} = -1.05$ V and -1.23 V explains why even at the fastest growth rate, the sample in case 'a' had a limited speed of 30.3 $\mu\text{m/s}$. Although similarly in case 'c' the shaded area shows a small fraction of each cycle, $V_{DC} = -1.15$ V is closer to -1.23 V than that in case 'a'. This may explain a slightly higher speed of 35.7 $\mu\text{m/s}$ at 83 mHz compare to case 'a'. As shown in Figure 25b, a much larger portion of each cycle covers the HEA mode with V_{DC} of -1.15 V. This can be the reason for achieving 55 $\mu\text{m/s}$ and 50 $\mu\text{m/s}$ at 71.5 mHz and 215 mHz, respectively. Figure 25d shows that due to V_{DC} of -1.25 V (being less than -1.23 V), more than 50% of each cycle is in the HEA mode. However, the growth rate in case 'd' never exceeded 37.5 $\mu\text{m/s}$. This is likely due to the lack of enough time in each cycle for releasing the hydrogen bubbles. Hence, the blockage of the electrode area with the stuck bubbles has limited the growth rate. In fact, the morphology of the samples through the SEM images shows larger variation in the pore sizes as evidence to the agglomeration of the hydrogen bubbles.

To understand the difference in the growth processes in different cases, the voltage variations vs. time are plotted for all four cases in Figure 26. Since water electrolysis at 1.23 V, the -1.23 V level is shown in the plots as a reference to the boundary for starting the hydrogen

evolution near the cathodes. It should be noted that, in practice, the transition between HEA and non-HEA mode is not a binary transition, but a strong electrolysis is expected at -1.23 V and lower. Hence, the part of the voltage in each cycle with a value less than -1.23 V is marked with a shaded triangle, indicating the expected HEA electroplating.

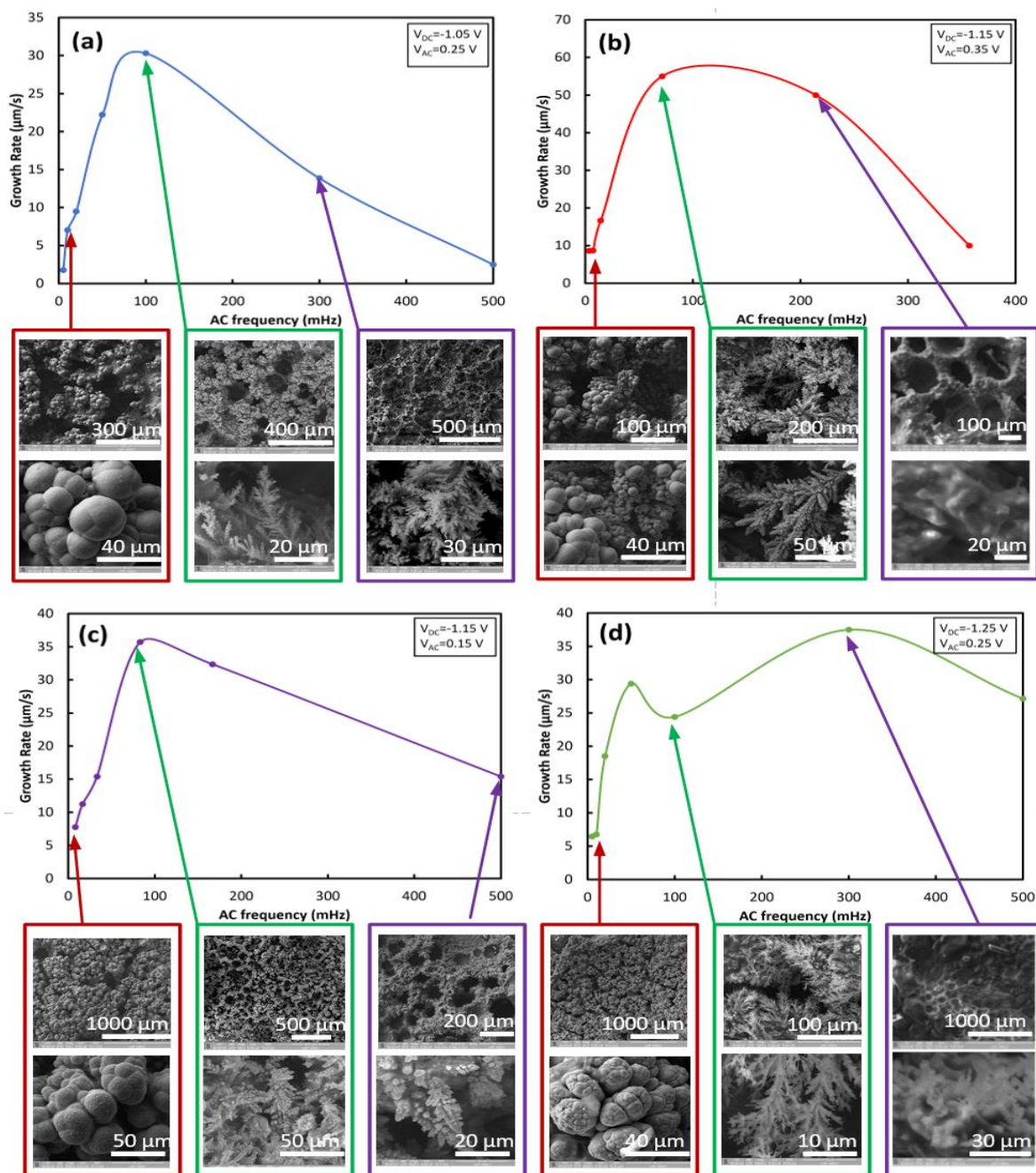


Figure 25. Selected SEM images of different samples associated to their growth conditions.

Case 'a' shows that, regardless of the frequency, HEA covers a small fraction of each cycle. Also, the large voltage difference between $V_{DC} = -1.05$ V and -1.23 V explains why even at the fastest growth rate, the sample in case 'a' had a limited speed of $30.3 \mu\text{m/s}$. Although similarly in case 'c' the shaded area shows a small fraction of each cycle, $V_{DC} = -1.15$ V is closer to -1.23 V. This may explain a slightly higher speed of $35.7 \mu\text{m/s}$ at 83 mHz compare to case 'a'. As shown in Figure 26b, a much larger portion of each cycle covers the HEA mode with V_{DC} of -1.15 V. This can be the reason for achieving $55 \mu\text{m/s}$ and $50 \mu\text{m/s}$ at 71.5 mHz and 215 mHz, respectively. Figure 26d shows that due to V_{DC} of -1.25 V (being less than -1.23 V), more than 50% of each cycle is in the HEA mode. However, the growth rate in case 'd' never exceeded $37.5 \mu\text{m/s}$. This is likely due to the lack of enough time in each cycle for releasing the hydrogen bubbles and blockage of the electrode area with the stuck bubbles. In fact, the morphology of the samples through the SEM images shows larger variation in the pore sizes as an evidence to the agglomeration of the hydrogen bubbles.

While the voltage profiles explain why case 'b' was preferred, for a better understanding of the frequency effect, we should consider the period of each cycle. As explained, low frequencies of 3 to 10 mHz are more like DC cases with the extended period of time staying in HEA and non-HEA modes. At higher frequencies of 500 mHz or near that, it takes only a few seconds for the voltage to switch back and forth between the HEA and non-HEA modes. Hence, the effect of switching between the two modes are not fully reflected in the results. Apparently, frequencies near 100 mHz which corresponds to 10 sec for each cycle are the best for achieving the fastest growth. Considering that a portion of each cycle is dedicated to the HEA mode, the results suggests that after a few seconds of HEA copper growth it is better to conduct the growth in a non-HEA mode for a few seconds to allow the generated bubbles leave the surface before their

agglomeration. Further study in this field is planned to characterize the electrical and mechanical properties of the electroplated coppers under different growth conditions. The results are expected to develop a practical recipe for controlling the electrodeposition process to achieve the highest growth rate and predictable micro and nano structures.

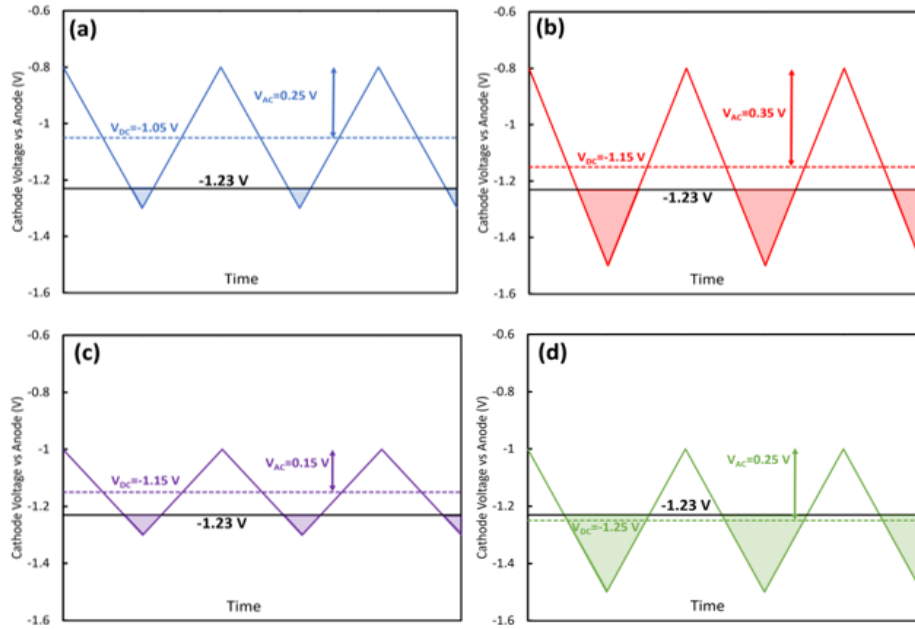


Figure 26. The voltage variation in cases ‘a’, ‘b’, ‘c’, and ‘d’. The shaded area on each curve shows the portion of each cycle at which the voltage of the cell exceeded the value required for the water electrolysis with strong HEA copper deposition.

7.4 Conclusion

Copper was successfully grown by the application of AC voltages without interrupting the mass transfer of the ions in solution. The constant interaction of the hydrogen bubbles restricts the complete deposition of copper which also creates a limitation in the movement of electrons from the bulk solution to the cations, not allowing the deposition of copper to take place for a longer period directly affecting the amount being deposited. It was reported that at frequencies near 100 mHz the fastest growth for copper electrodeposition was achieved.

As show in the results after the deposition of copper is conducted in a HEA mode, it's better to conduct the copper growth in a non-HEA mode for a few seconds to allow the released of the hydrogen bubbles from the surface of the printed circuit board to avoid their agglomeration and the limitation of copper deposition.

Chapter 8: Conclusion and Suggestions for Future Work

8.1 Conclusion

A variety of projects have been addressed through out this dissertation to understand the copper electrodeposition technique, to enhance the growth rate by the implementation of the hydrogen evolution mechanism and to improve the capability of a variety of substrates by the implementation of a technique that allows flexibility, more surface area with less consumption of material and a variation in morphologies for broader applications. The fundamental study of this work focused on a redox reaction among CuSO_4 and H_2SO_4 which takes place at the electrochemical cell in the copper electrodeposition process which by surpassing electrolysis used the hydrogen bubble release as an advantage to improve the convection of the copper ions towards the cathode to enhance the growth rate of the copper being deposited. The rapid growth rate of copper via electrodeposition is a promising approach for improving the existing techniques, reducing the time of production, and allowing the growth of a low-cost technique with a significant opportunity to employ new applications. The research conducted in this dissertation has contributed to redesign and improve the copper electrodeposition procedure by using in our favor the electrolysis to obtain better morphological structures which can be modified by the specific application of the combination of voltage and scan rate, better conductivity, and promising growth rate. Significant contribution has been made by:

- Improving the growth rate of copper for printing a circuit layout. The high growth rate was achieved due to HEA electroplating method which can be used in the future for developing a copper printing method.

- It has been shown that the acid and CuSO_4 have a direct effect on the lateral copper growth. A concentration of 1.0M and 1.5 M of acid is ideal to obtain a faster growth rate and great copper formation over the substrate.
- By the application of AC voltages the copper electrodeposition technique was achieved without the restriction of hydrogen evolution bubbles over the surface by conducting the copper growth in a non-HEA mode for a few seconds to allow the released of the hydrogen bubbles from the surface which prevents the agglomerations and coalescence of bubbles and allows a continuous growth of copper.
- It was shown that copper electrodeposition over fabrics is a viable method which does not require any soldering machine, preventing the damage of the fabrics and achieving a proper metal deposition facilitating the commercialization and development of several applications.

8.2 Future Work

8.2.1 Triaxial Braided Piezo Electric Fibers

Further study is needed to understand and enhance the application of copper electrodeposition over triaxial braided piezo fiber metallization to enhance piezoelectricity performance of the triaxial braided energy harvester by applying hydrogen evolution assisted (HEA) electroplating. In previous work the triaxial braided PVDF yarn as seen in Figure 27a and 27b has shown extreme durability with no changes in its performance. Further studies showed some reduction in the flexibility of the structure after the copper deposition as shown in Figure 27c and 27d demonstrating the need for further studies to improve fiber flexibility for a wider range of applications.

The developed triaxial piezoelectric energy generator can be easily fabricated with unlimited lengths to meet specific energy and power needs. In addition, the triaxial braided structure provides more durability for the piezoelectric energy generator device due to novel packaging which could protect the PVDF fibers and silver coated nylon electrodes in the device [86].



Figure 27. a) Triaxial braided piezo fiber, b) braided PVDF with inner silver coated nylon, c) triaxial braided piezo fiber with MWCNTs ink used for the hydrogen evolution assisted electroplating showing a higher porosity structure, d) triaxial braided piezo fiber without MWCNTs after deposition

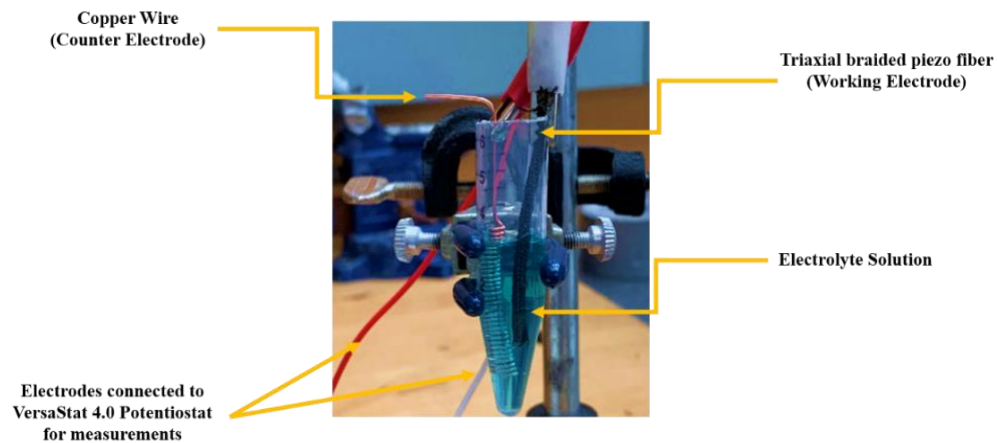


Figure 28. Schematic of the electrochemical cell. Both working and counter electrodes were connected to the VersaStat 4.0 potentiostat for measurements.

Improvement of the set-up for copper electrodeposition over triaxial braided piezo fiber is needed to enhance the visibility while the experiment takes place and to record the procedure for further studies.

8.2.2 Incorporation of Conductive Fibers over Textiles to Improve Flexibility and Conduct Copper Electrodeposition

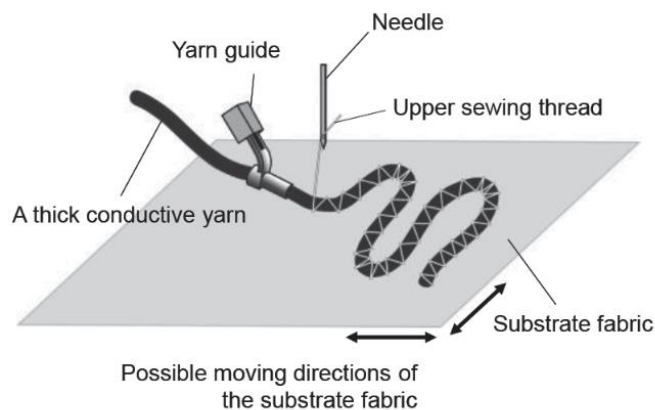


Figure 29. Integration of fibers on a flexible substrate (fabric or polymer) to conduct the copper electroplating technique [67]

Electrospinning fibers can directly be collected in the substrate (polymer or fabric) to perform copper electrodeposition for interconnection development. Also the integration of triaxial fibers by sewing them using conductive or non-conductive thread (depending on the conductivity of the fiber being used) to the fabric or polymer is another technique that can be conducted to perform copper electrodeposition over them and then cover the substrate and the fiber with a polymer that will provide flexibility and that is washable.

8.2.3 Nozzle for Direct Copper Electrodeposition

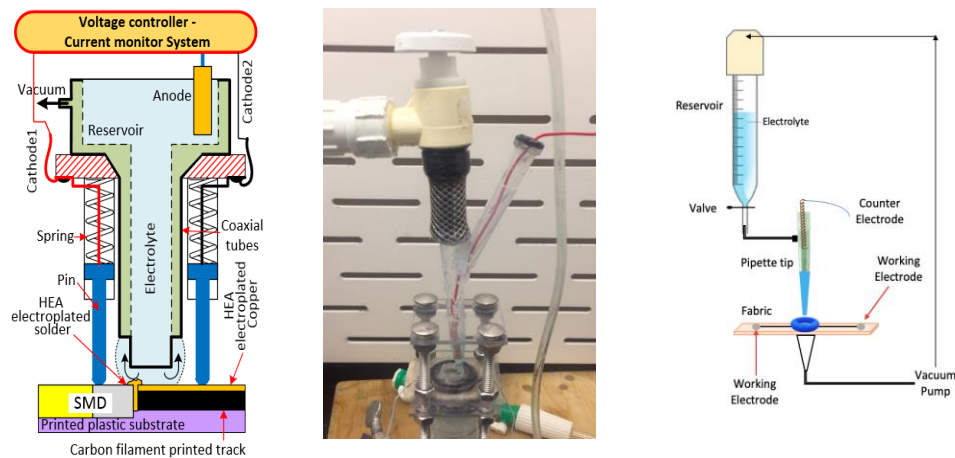


Figure 30. Nozzle Set-up

- Enhancement of the nozzle set up is needed for continuous and copper electrodeposition over fabrics without the interruption of the procedure.
- Prevention of electrolyte derrames is needed
- Determine the voltage for each fabric is needed
- Enhancement of the set up base is needed to allow the movement from x and y in order to obtain continuous deposition along the whole fabric without stopping the procedure.

References

- [1] J. G. Kaufmann *et al.*, “Megasonic agitation for enhanced electrodeposition of copper,” *Microsyst. Technol.*, vol. 15, no. 8, pp. 1245–1254, 2009, doi: 10.1007/s00542-009-0886-2.
- [2] S. Costello *et al.*, “Electrodeposition of copper into high aspect ratio PCB micro-via using megasonic agitation,” *Microsyst. Technol.*, vol. 19, no. 6, pp. 783–790, 2013, doi: 10.1007/s00542-013-1746-7.
- [3] M. A. Pasquale, L. M. Gassa, and A. J. Arvia, “Copper electrodeposition from an acidic plating bath containing accelerating and inhibiting organic additives,” *Electrochim. Acta*, vol. 53, no. 20, pp. 5891–5904, Aug. 2008, doi: 10.1016/j.electacta.2008.03.073.
- [4] A. A. Pasa and W. Schwarzacher, “Electrodeposition of thin films and multilayers on silicon,” *Phys. Status Solidi Appl. Res.*, vol. 173, no. 1, pp. 73–84, 1999, doi: 10.1002/(SICI)1521-396X(199905)173:1<73::AID-PSSA73>3.0.CO;2-8.
- [5] S. M. Rosa-Ortiz, F. Khorramshahi, and A. Takshi, “Study the impact of CuSO₄ and H₂SO₄ concentrations on lateral growth of hydrogen evolution assisted copper electroplating,” *J. Appl. Electrochem.*, vol. 49, no. 12, pp. 1203–1210, 2019, doi: 10.1007/s10800-019-01359-2.
- [6] E. Vaněčková *et al.*, “Copper electroplating of 3D printed composite electrodes,” *J. Electroanal. Chem.*, vol. 858, p. 113763, 2020, doi: 10.1016/j.jelechem.2019.113763.
- [7] “Electroplating Market - Forecasts from 2020 to 2025.” <https://www.researchandmarkets.com/reports/4986721/electroplating-market-forecasts-from-2020-to> (accessed Apr. 08, 2020).
- [8] “The World Copper Market: Structure and Econometric Model - G. Wagenhals - Google Books.” [https://books.google.com/books?id=Dp_wCAAAQBAJ&printsec=frontcover&dq=The+world+copper+market+:+structure+and+econometric+model.&hl=en&newbks=1&newbks_redir=0&sa=X&ved=2ahUKEwjcltTJ4dnoAhWFZd8KHftVAg4Q6AEwAHoECAUQAg#v=onepage&q=The world copper market %3A structure and econometric model.&f=false](https://books.google.com/books?id=Dp_wCAAAQBAJ&printsec=frontcover&dq=The+world+copper+market+:+structure+and+econometric+model.&hl=en&newbks=1&newbks_redir=0&sa=X&ved=2ahUKEwjcltTJ4dnoAhWFZd8KHftVAg4Q6AEwAHoECAUQAg#v=onepage&q=The%20world%20copper%20market%20%3A%20structure%20and%20econometric%20model.&f=false) (accessed Apr. 08, 2020).
- [9] S. Miura and H. Honma, “Advanced copper electroplating for application of electronics,” *Surf. Coatings Technol.*, vol. 169–170, pp. 91–95, 2003, doi: 10.1016/S0257-8972(03)00165-8.
- [10] T. Kobayashi, J. Kawasaki, K. Mihara, and H. Honma, “Via-filling using electroplating for build-up PCBs,” vol. 47, pp. 85–89, 2001.
- [11] W. A. D. M. Jayathilaka *et al.*, “Significance of Nanomaterials in Wearables: A Review on Wearable Actuators and Sensors,” *Adv. Mater.*, vol. 31, no. 7, pp. 1–21, 2019, doi: 10.1002/adma.201805921.

- [12] D. P. Dubal, N. R. Chodankar, D. H. Kim, and P. Gomez-Romero, "Towards flexible solid-state supercapacitors for smart and wearable electronics," *Chem. Soc. Rev.*, vol. 47, no. 6, pp. 2065–2129, 2018, doi: 10.1039/c7cs00505a.
- [13] L. Huang, D. Santiago, P. Loyselle, and L. Dai, "Graphene-Based Nanomaterials for Flexible and Wearable Supercapacitors," *Small*, vol. 14, no. 43, p. 1800879, Oct. 2018, doi: 10.1002/sml.201800879.
- [14] S. Kasap, *Principles of electronic materials and devices*. McGraw-Hill, 2006.
- [15] N. D. Nikolić, L. J. Pavlović, M. G. Pavlović, and K. I. Popov, "Formation of dish-like holes and a channel structure in electrodeposition of copper under hydrogen co-deposition," *Electrochim. Acta*, vol. 52, no. 28, pp. 8096–8104, 2007, doi: 10.1016/j.electacta.2007.07.008.
- [16] S. M. Rosa-Ortiz, K. K. Kadari, and A. Takshi, "Low Temperature Soldering Surface-Mount Electronic Components with Hydrogen Assisted Copper Electroplating," *MRS Adv.*, vol. 3, no. 18, pp. 963–968, 2018, doi: 10.1557/adv.2017.641.
- [17] B. Cortese, D. Caschera, G. Padeletti, G. M. Ingo, and G. Gigli, "A brief review of surface-functionalized cotton fabrics," *Surf. Innov.*, vol. 1, no. 3, pp. 140–156, 2013, doi: 10.1680/si.13.00008.
- [18] C. Hamann, A. Hamnett, and W. Vielstich, *Electrochemistry*, 2nd editio. Wiley-VCH Verlag, 2007.
- [19] N. D. Nikolić and G. Branković, "Effect of parameters of square-wave pulsating current on copper electrodeposition in the hydrogen co-deposition range," *Electrochem. commun.*, vol. 12, no. 6, pp. 740–744, 2010, doi: 10.1016/j.elecom.2010.03.021.
- [20] N. D. Nikolić, G. Branković, M. G. Pavlović, and K. I. Popov, "The effect of hydrogen co-deposition on the morphology of copper electrodeposits. II. Correlation between the properties of electrolytic solutions and the quantity of evolved hydrogen," *J. Electroanal. Chem.*, vol. 621, no. 1, pp. 13–21, 2008, doi: 10.1016/j.jelechem.2008.04.006.
- [21] N. D. Nikolić, K. I. Popov, L. J. Pavlović, and M. G. Pavlović, "Phenomenology of a formation of a honeycomb-like structure during copper electrodeposition," *J. Solid State Electrochem.*, vol. 11, no. 5, pp. 667–675, 2007, doi: 10.1007/s10008-006-0222-z.
- [22] A. J. Bard and L. R. Faulkner, *Electrochemical Methods: Fundamentals and applications*, Second Edi., vol. 2. John Wiley & Sons, Inc., 2001.
- [23] N. D. Nikolić and G. Branković, "Comparison of open porous copper structures obtained by the different current regimes of electrolysis," *Mater. Lett.*, vol. 70, pp. 11–15, Mar. 2012, doi: 10.1016/j.matlet.2011.11.081.
- [24] M. S. Chandrasekar and M. Pushpavanam, "Pulse and pulse reverse plating-Conceptual, advantages and applications," *Electrochim. Acta*, vol. 53, no. 8, pp. 3313–3322, 2008, doi: 10.1016/j.electacta.2007.11.054.
- [25] K. I. Popov and M. D. Maksimović, "Theory of the Effect of Electrodeposition at a Periodically Changing Rate on the Morphology of Metal Deposits," no. 1, pp. 193–250, 1989, doi: 10.1007/978-1-4684-8667-4_3.
- [26] K. I. Popov, M. D. Maksimović, J. D. Trnjančev, and M. G. Pavlović, "Dendritic electrocrystallization and the mechanism of powder formation in the potentiostatic electrodeposition of metals," *J. Appl. Electrochem.*, vol. 11, no. 2, pp. 239–246, 1981, doi: 10.1007/BF00610985.

- [27] K. I. Popov, D. N. Keča, S. I. Vidojković, B. J. Lazarević, and V. B. Milojković, “Mathematical model and digital simulation of pulsating overpotential copper electrodeposition,” *J. Appl. Electrochem.*, vol. 6, no. 4, pp. 365–370, 1976, doi: 10.1007/BF00608923.
- [28] Y.-M. Byoun, Y.-T. Noh, Y.-G. Kim, S.-H. Ma, and G.-H. Kim, “Characterization of Pulse Reverses Electroforming on Hard Gold Coating,” *J. Nanosci. Nanotechnol.*, vol. 18, no. 3, pp. 2104–2108, 2017, doi: 10.1166/jnn.2018.14937.
- [29] N. D. Nikolić, V. M. Maksimović, M. G. Pavlović, and K. I. Popov, “Cross-section analysis of the morphology of electrodeposited copper obtained in the hydrogen co-deposition range | Russian Source,” *J. Serbian Chem. Soc.*, vol. 74, no. 6, pp. 689–696, 2009, doi: 10.2298/JSC0906689N.
- [30] K. I. Popov, M. D. Maksimović, and B. M. Ocko, “Fundamental Aspects of Pulsating Current Metal Electrodeposition I. The effect of the pulsating current on the surface roughness and the porosity of metal deposits,” vol. 11, pp. 99–109, 1980.
- [31] K. I. Popov, M. D. Spasojevic, M. D. . Maksimović, and I. S. Boskovic, “Fundamental aspects of pulsating current metal electrodeposition II: The mechanism of metal film formation on an inert electrode,” *Surf. Technol.*, vol. 11, pp. 111–116, 1980.
- [32] K. I. Popov, M. D. Maksimović, and S. S. Djokic, “Fundamental Aspects of Pulsating Current Metal Electrodeposition III. Maximum practical deposition rate,” *Surf. Technol.*, vol. 14, pp. 323–333, 1981.
- [33] K. I. Popov and M. D. Maksimović, “Fundamental Aspects of Pulsating Current Metal Electrodeposition IV: Tafel Equation in the deposition of metals by a pulsating current,” vol. 15, pp. 161–165, 1982.
- [34] M. D. Maksimović and Z. S. Dimitrijević, “Fundamental aspects of pulsating current metal electrodeposition V: The determination of the optimal frequency range,” *Surf. Technol.*, vol. 17, no. 1, pp. 3–9, 1982, doi: 10.1016/0376-4583(82)90055-3.
- [35] K. I. Popov, M. D. Maksimović, and D. Č. Totovski, “Fundamental aspects of pulsating current metal electrodeposition VI: The comparison of electrode surface roughening in pulsating current and periodic reverse current electrodeposition of metals,” *Surf. Technol.*, vol. 17, no. 2, pp. 125–129, 1982, doi: 10.1016/0376-4583(82)90014-0.
- [36] L. R. Barstad, T. Buckley, R. Cruz, and T. Goodrick, “Reverse pulse plating composition and method,” 2004.
- [37] P. Leisner, M. Fredenberg, and I. Belov, “Pulse and pulse reverse plating of copper from acid sulphate solutions,” *Trans. Inst. Met. Finish.*, vol. 88, no. 5, pp. 243–247, 2010, doi: 10.1179/002029610X12791981507721.
- [38] S. Cherevko, N. Kulyk, and C. H. Chung, “Pulse-reverse electrodeposition for mesoporous metal films: Combination of hydrogen evolution assisted deposition and electrochemical dealloying,” *Nanoscale*, vol. 4, no. 2, pp. 568–575, 2012, doi: 10.1039/c1nr11503k.
- [39] M. B. How and N. Aziz, “Influences of magnetic field on the fractal morphology in copper electrodeposition,” vol. 285, p. 12021, 2018, doi: 10.1088/1757-899X/285/1/012021.
- [40] D. Fernández, Z. Diao, P. Dunne, and J. M. D. Coey, “Influence of magnetic field on hydrogen reduction and co-reduction in the Cu/CuSO₄ system,” *Electrochim. Acta*, vol. 55, no. 28, pp. 8664–8672, 2010, doi: 10.1016/j.electacta.2010.08.004.
- [41] H. C. Shin, J. Dong, and M. Liu, “Nanoporous Structures Prepared by an Electrochemical Deposition Process,” *Adv. Mater.*, vol. 15, no. 19, pp. 1610–1614, 2003, doi: 10.1002/adma.200305160.

- [42] N. D. Nikolić, G. Branković, V. M. Maksimović, M. G. Pavlović, and K. I. Popov, "Influence of potential pulse conditions on the formation of honeycomb-like copper electrodes," *J. Electroanal. Chem.*, vol. 635, no. 2, pp. 111–119, 2009, doi: 10.1016/j.jelechem.2009.08.005.
- [43] N. D. Nikolic, K. I. Popov, L. J. Pavlovic, and M. G. Pavlovic, "Determination of critical conditions for the formation of electrodeposited copper structures suitable for electrodes in electrochemical devices," *Sensors*, vol. 7, no. 1, pp. 1–15, 2007, doi: 10.3390/s7010001.
- [44] J. Ainsworth, D. Disher, and D. Morreal, "Desktop 3D Printer Opus Citation," 2015, [Online]. Available: http://opus.ipfw.edu/etcs_seniorproj_mctid%0Ahttp://opus.ipfw.edu/etcs_seniorproj_mce tid/277.
- [45] E. A. Rojas-Nastrucci, A. D. Snider, and T. M. Weller, "Propagation Characteristics and Modeling of Meshed Ground Coplanar Waveguide," *IEEE Trans. Microw. Theory Tech.*, vol. 64, no. 11, pp. 3460–3468, 2016, doi: 10.1109/TMTT.2016.2606409.
- [46] S. Ready, F. Endicott, G. L. Whiting, T. N. Ng, E. M. Chow, and J. Lu, "3D Printed Electronics."
- [47] H. H. Lee, K. Sen Chou, and K. C. Huang, "Inkjet printing of nanosized silver colloids," *Nanotechnology*, vol. 16, no. 10, pp. 2436–2441, 2005, doi: 10.1088/0957-4484/16/10/074.
- [48] "Copper Electrodeposition on Textile for Wearable Electronics - IOPscience." <https://iopscience.iop.org/article/10.1149/MA2019-02/16/950> (accessed Apr. 08, 2020).
- [49] F. A. Lowenheim and S. Senderoff, *Modern Electroplating*. Wiley & Sons Inc., 1964.
- [50] N. D. Nikolić, L. J. Pavlović, M. G. Pavlović, and K. I. Popov, "Effect of temperature on the electrodeposition of disperse copper deposits," *J. Serbian Chem. Soc.*, vol. 72, no. 12, pp. 1369–1381, 2007, doi: 10.2298/JSC0712369N.
- [51] N. D. Nikoli, K. I. Popov, L. J. Pavlovi, and M. G. Pavlovi, "Morphologies of copper deposits obtained by the electrodeposition at high overpotentials," vol. 201, pp. 560–566, 2006, doi: 10.1016/j.surfcoat.2005.12.004.
- [52] L. Huang, E. S. Lee, and K. B. Kim, "Electrodeposition of monodisperse copper nanoparticles on highly oriented pyrolytic graphite electrode with modulation potential method," *Colloids Surfaces A Physicochem. Eng. Asp.*, vol. 262, no. 1–3, pp. 125–131, 2005, doi: 10.1016/j.colsurfa.2005.03.023.
- [53] V. S. Donepudi, R. Venkatachalapathy, P. O. Ozemoyah, C. S. Johnson, and J. Prakash, "Electrodeposition of Copper from Sulfate Electrolytes: Effects of Thiourea on Resistivity and Electrodeposition Mechanism of Copper," *Electrochem. Solid-State Lett.*, vol. 4, no. 2, p. C13, 2001, doi: 10.1149/1.1342144.
- [54] N. D. Nikolić, K. I. Popov, L. J. Pavlović, and M. G. Pavlović, "The effect of hydrogen codeposition on the morphology of copper electrodeposits. I. the concept of effective overpotential," *J. Electroanal. Chem.*, vol. 588, no. 1, pp. 88–98, 2006, doi: 10.1016/j.jelechem.2005.12.006.
- [55] N. Jäckel *et al.*, "Anomalous or regular capacitance? The influence of pore size dispersity on double-layer formation," *J. Power Sources*, vol. 326, pp. 660–671, 2016, doi: 10.1016/j.jpowsour.2016.03.015.

- [56] “Adhesion Measurement Methods: Theory and Practice - Robert Lacombe - Google Books.”
[https://books.google.com/books?hl=en&lr=&id=oEluBwAAQBAJ&oi=fnd&pg=PP1&dq=Lacombe+R+\(2005\)+Adhesion+measurement+methods:+theory+and+practice.+CRC+Press,+Boca+Raton&ots=PM2b_cRotw&sig=EvuTx73GoVphwZ-HHKJ_CqIDcf8#v=onepage&q=Lacombe R \(2005\) Adhesion measurement methods%3A theory and practice. CRC Press%2C Boca Raton&f=false](https://books.google.com/books?hl=en&lr=&id=oEluBwAAQBAJ&oi=fnd&pg=PP1&dq=Lacombe+R+(2005)+Adhesion+measurement+methods:+theory+and+practice.+CRC+Press,+Boca+Raton&ots=PM2b_cRotw&sig=EvuTx73GoVphwZ-HHKJ_CqIDcf8#v=onepage&q=Lacombe R (2005) Adhesion measurement methods%3A theory and practice. CRC Press%2C Boca Raton&f=false) (accessed Apr. 10, 2020).
- [57] T. D. A. Jones, A. Bernassau, D. Flynn, D. Price, M. Beadel, and M. P. Y. Desmulliez, “Copper electroplating of PCB interconnects using megasonic acoustic streaming,” *Ultrason. Sonochem.*, vol. 42, no. November 2017, pp. 434–444, 2018, doi: 10.1016/j.ultsonch.2017.12.004.
- [58] S. S. Djokic and |, *MODERN ASPECTS OF ELECTROCHEMISTRY, No. 48: ELECTRODEPOSITION THEORY AND PRACTICE*. 2010.
- [59] H. Matsushima, T. Iida, and Y. Fukunaka, “Gas bubble evolution on transparent electrode during water electrolysis in a magnetic field,” *Electrochim. Acta*, vol. 100, pp. 261–264, 2013, doi: 10.1016/j.electacta.2012.05.082.
- [60] G. V. G. Mercado, C. J. González, M. I. Oliva, V. Brunetti, and G. A. Eimer, “Morphology of Copper Deposits Obtained by Metallic Electrodeposition,” *Procedia Mater. Sci.*, vol. 8, pp. 635–640, 2015, doi: 10.1016/j.mspro.2015.04.119.
- [61] J. Foroughi, T. Mitew, P. Ogunbona, R. Raad, and F. Safaei, “Smart Fabrics and Networked Clothing: Recent developments in CNT-based fibers and their continual refinement.,” *IEEE Consum. Electron. Mag.*, vol. 5, no. 4, pp. 105–111, Oct. 2016, doi: 10.1109/MCE.2016.2590220.
- [62] T. R. Ray *et al.*, “Bio-integrated wearable systems: A comprehensive review,” *Chemical Reviews*, vol. 119, no. 8. American Chemical Society, pp. 5461–5533, Apr. 24, 2019, doi: 10.1021/acs.chemrev.8b00573.
- [63] A. Takshi and S. M. Rosa-Ortiz, “Electrochemical Three-Dimensional Printing and Soldering,” US 2019 / 0017185 A1, 2019.
- [64] M. Stoppa and A. Chiolerio, “Wearable electronics and smart textiles: A critical review,” *Sensors (Switzerland)*, vol. 14, no. 7, pp. 11957–11992, 2014, doi: 10.3390/s140711957.
- [65] B. Aljafari, T. Alamro, M. K. Ram, and A. Takshi, “Polyvinyl alcohol-acid redox active gel electrolytes for electrical double-layer capacitor devices,” *J. Solid State Electrochem.*, vol. 23, no. 1, pp. 125–133, Jan. 2019, doi: 10.1007/s10008-018-4120-y.
- [66] L. M. Castano and A. B. Flatau, “Smart fabric sensors and e-textile technologies: a review,” *Smart Mater. Struct.*, vol. 23, no. 5, p. 053001, Apr. 2014, doi: 10.1088/0964-1726/23/5/053001.
- [67] J.-S. Roh, “Conductive Yarn Embroidered Circuits for System on Textiles,” *Wearable Technol.*, 2018, doi: 10.5772/intechopen.76627.
- [68] I. Locher, “Technologies for system-on-textile integration,” 2006.
- [69] M. Gao, L. Li, and Y. Song, “Inkjet printing wearable electronic devices,” *J. Mater. Chem. C*, vol. 5, no. 12, pp. 2971–2993, 2017, doi: 10.1039/c7tc00038c.
- [70] L. Buechley and M. Eisenberg, “Fabric PCBs, electronic sequins, and socket buttons: Techniques for e-textile craft,” *Pers. Ubiquitous Comput.*, vol. 13, no. 2, pp. 133–150, 2009, doi: 10.1007/s00779-007-0181-0.

- [71] J. Kim, R. Kumar, A. J. Bhandodkar, and J. Wang, “Advanced Materials for Printed Wearable Electrochemical Devices: A Review,” *Adv. Electron. Mater.*, vol. 3, no. 1, 2017, doi: 10.1002/aelm.201600260.
- [72] S. Jang *et al.*, “Sintering of inkjet printed copper nanoparticles for flexible electronics,” *Scr. Mater.*, vol. 62, no. 5, pp. 258–261, 2010, doi: 10.1016/j.scriptamat.2009.11.011.
- [73] E. Ismar, S. Kurşun Bahadır, F. Kalaoglu, and V. Koncar, “Futuristic Clothes: Electronic Textiles and Wearable Technologies,” *Glob. Challenges*, vol. 4, no. 7, p. 1900092, 2020, doi: 10.1002/gch2.201900092.
- [74] Q. Shi *et al.*, “Progress in wearable electronics/photronics—Moving toward the era of artificial intelligence and internet of things,” *InfoMat*, vol. 2, no. 6, pp. 1131–1162, 2020, doi: 10.1002/inf2.12122.
- [75] P. C. Y. Chow and T. Someya, “Organic Photodetectors for Next-Generation Wearable Electronics,” *Adv. Mater.*, vol. 32, no. 15, pp. 1–26, 2020, doi: 10.1002/adma.201902045.
- [76] W. Zeng, L. Shu, Q. Li, S. Chen, F. Wang, and X. M. Tao, “Fiber-based wearable electronics: A review of materials, fabrication, devices, and applications,” *Adv. Mater.*, vol. 26, no. 31, pp. 5310–5336, 2014, doi: 10.1002/adma.201400633.
- [77] J. Lee, B. Llerena Zambrano, J. Woo, K. Yoon, and T. Lee, “Recent Advances in 1D Stretchable Electrodes and Devices for Textile and Wearable Electronics: Materials, Fabrications, and Applications,” *Adv. Mater.*, vol. 32, no. 5, pp. 1–28, 2020, doi: 10.1002/adma.201902532.
- [78] H. Liu *et al.*, “Paper: A promising material for human-friendly functional wearable electronics,” *Mater. Sci. Eng. R Reports*, vol. 112, pp. 1–22, 2017, doi: 10.1016/j.mser.2017.01.001.
- [79] S. M. Rosa-Ortiz and A. Takshi, “Copper Electrodeposition by Hydrogen Evolution Assisted Electroplating (HEA) for Wearable Electronics,” *2020 Pan Pacific Microelectron. Symp. Pan Pacific 2020*, 2020, doi: 10.23919/PanPacific48324.2020.9059338.
- [80] C. Wang, K. Xia, H. Wang, X. Liang, Z. Yin, and Y. Zhang, “Advanced Carbon for Flexible and Wearable Electronics,” *Adv. Mater.*, vol. 31, no. 9, pp. 1–37, 2019, doi: 10.1002/adma.201801072.
- [81] Z. Tang *et al.*, “Highly conductive, washable and super-hydrophobic wearable carbon nanotubes e-textile for vacuum pressure sensors,” *Sensors Actuators, A Phys.*, vol. 303, p. 111710, 2020, doi: 10.1016/j.sna.2019.111710.
- [82] D. R. Gabe and A. J. Cobley, “Catalytic anodes for electrodeposition: A study for acid copper printed circuit board (PCB) production,” *Circuit World*, vol. 32, no. 3, pp. 3–10, 2006, doi: 10.1108/03056120610663353.
- [83] L. Yin, Z. H. Liu, Z. P. Yang, Z. L. Wang, and S. Shingubara, “Effect of PEG molecular weight on bottom-up filling of copper electrodeposition for PCB interconnects,” *Trans. Inst. Met. Finish.*, vol. 88, no. 3, pp. 149–153, 2010, doi: 10.1179/174591910X12692711390390.
- [84] Y. F. Guimarães, I. D. Santos, and A. J. B. Dutra, “Direct recovery of copper from printed circuit boards (PCBs) powder concentrate by a simultaneous electroleaching-electrodeposition process,” *Hydrometallurgy*, vol. 149, pp. 63–70, 2014, doi: 10.1016/j.hydromet.2014.06.005.
- [85] A. J. Cobley and D. R. Gabe, “Characterisation of insoluble anodes for acid copper electrodeposition,” *Trans. Inst. Met. Finish.*, vol. 81, no. 2, pp. 37–44, 2003, doi: 10.1080/00202967.2003.11871487.

- [86] F. Mokhtari, J. Foroughi, T. Zheng, Z. Cheng, and G. M. Spinks, “Triaxial braided piezo fiber energy harvesters for self-powered wearable technologies,” *J. Mater. Chem. A*, vol. 7, no. 14, pp. 8245–8257, 2019, doi: 10.1039/c8ta10964h.

Appendix A: Copyright Permissions

The permission below is for the use of Figures 2 to 5 from Chapter 3, Figures 6 to 12 from Chapter 4, and Table 4 and Figures 17 to 21 from Chapter 6.

Author reuse

Please check the Copyright Transfer Statement (CTS) or Licence to Publish (LTP) that you have signed with Springer Nature to find further information about the reuse of your content.

Authors have the right to reuse their article's Version of Record, in whole or in part, in their own thesis. Additionally, they may reproduce and make available their thesis, including Springer Nature content, as required by their awarding academic institution. Authors must properly cite the published article in their thesis according to current citation standards.

Material from: 'AUTHOR, TITLE, JOURNAL TITLE, published [YEAR], [publisher - as it appears on our copyright page]'

If you are in any doubt about whether your intended re-use is covered, please contact journalpermissions@springernature.com for confirmation.

The permission below is for the use of Table 3 and Figures 13 to 16 from Chapter 5.



IEEE
Requesting permission to reuse content from an IEEE publication

Copper Electrodeposition by Hydrogen Evolution Assisted Electroplating (HEA) for Wearable Electronics
Conference Proceedings: 2020 Pan Pacific Microelectronics Symposium (Pan Pacific)
Author: Sabrina M. Rosa-Ortiz
Publisher: IEEE
Date: Feb. 2020
Copyright © 2020, IEEE

Thesis / Dissertation Reuse

The IEEE does not require individuals working on a thesis to obtain a formal reuse license, however, you may print out this statement to be used as a permission grant:

Requirements to be followed when using any portion (e.g., figure, graph, table, or textual material) of an IEEE copyrighted paper in a thesis:

- 1) In the case of textual material (e.g., using short quotes or referring to the work within these papers) users must give full credit to the original source (author, paper, publication) followed by the IEEE copyright line © 2011 IEEE.
- 2) In the case of illustrations or tabular material, we require that the copyright line © [Year of original publication] IEEE appear prominently with each reprinted figure and/or table.
- 3) If a substantial portion of the original paper is to be used, and if you are not the senior author, also obtain the senior author's approval.

Requirements to be followed when using an entire IEEE copyrighted paper in a thesis:

- 1) The following IEEE copyright/ credit notice should be placed prominently in the references: © [year of original publication] IEEE. Reprinted, with permission, from [author names, paper title, IEEE publication title, and month/year of publication]
- 2) Only the accepted version of an IEEE copyrighted paper can be used when posting the paper or your thesis on-line.
- 3) In placing the thesis on the author's university website, please display the following message in a prominent place on the website: In reference to IEEE copyrighted material which is used with permission in this thesis, the IEEE does not endorse any of [university/educational entity's name goes here]'s products or services. Internal or personal use of this material is permitted. If interested in reprinting/republishing IEEE copyrighted material for advertising or promotional purposes or for creating new collective works for resale or redistribution, please go to http://www.ieee.org/publications_standards/publications/rights/rights_link.html to learn how to obtain a License from RightsLink.

If applicable, University Microfilms and/or ProQuest Library, or the Archives of Canada may supply single copies of the dissertation.

[BACK](#) [CLOSE WINDOW](#)

The permission below is for the use of Figures 22 to 26 from Chapter 7.

Author rights

The below table explains the rights that authors have when they publish with Elsevier, for authors who choose to publish either open access or subscription. These apply to the corresponding author and all co-authors.

Author rights in Elsevier's proprietary Journals	Published open access	Published subscription
Retain patent and trademark rights	√	√
Retain the rights to use their research data freely without any restriction	√	√
Receive proper attribution and credit for their published work	√	√
Re-use their own material in new works without permission or payment (with full acknowledgement of the original article): 1. Extend an article to book length 2. Include an article in a subsequent compilation of their own work 3. Re-use portions, excerpts, and their own figures or tables in other works.	√	√
Use and share their works for scholarly purposes (with full acknowledgement of the original article): 1. In their own classroom teaching. Electronic and physical distribution of copies is permitted 2. If an author is speaking at a conference, they can present the article and distribute copies to the attendees 3. Distribute the article, including by email, to their students and to research colleagues who they know for their personal use 4. Share and publicize the article via Share Links, which offers 50 days' free access for anyone, without signup or registration 5. Include in a thesis or dissertation (provided this is not published commercially) 6. Share copies of their article privately as part of an invitation-only work group on commercial sites with which the publisher has a hosting agreement	√	√
Publicly share the preprint on any website or repository at any time.	√	√
Publicly share the accepted manuscript on non-commercial sites	√	√ using a CC BY-NC-ND license and usually only after an embargo period (see Sharing Policy for more information)
Publicly share the final published article	√ in line with the author's choice of end user license	x
Retain copyright	√	x

The permission below is for the use of Figures 29 from Chapter 8.